arXiv:1606.07117v1 [astro-ph.SR] 22 Jun 2016

Boron Abundances Across the "Li-Be Dip" in the Hyades Cluster[1]

Ann Merchant Boesgaard[1], Michael G. Lum[1]

Institute for Astronomy, University of Hawai'i at Manoa, 2680 Woodlawn Drive, Honolulu, HI 96822

boes@ifa.hawaii.edu

mikelum@ifa.hawaii.edu

Constantine P. Deliyannis

Department of Astronomy, Indiana University, 727 East 3rd Street, Swain Hall West 319, Bloomington, IN 47405-7105

cdeliyan@indiana.edu

Jeremy R. King[1]

Department of Physics and Astronomy, Clemson University, 118 Kinard Laboratory of Physics, Clemson, SC 29634-0978

jking2@clemson.edu

Marc H. Pinsonneault, & Garrett Somers

Department of Astronomy, The Ohio State University, 140 West 18th Avenue, Columbus, OH 43210

pinsonneault.1@osu.edu

somers@astronomy.ohio-state.edu

ABSTRACT

Dramatic deficiencies of Li in the mid-F dwarf stars of the Hyades cluster were discovered by Boesgaard & Tripicco. Boesgaard & King discovered corresponding, but smaller, deficiencies in Be in the same narrow temperature region

[1]Visiting Astronomer, W. M. Keck Observatory jointly operated by the California Institute of Technology and the University of California.

in the Hyades. With the Space Telescope Imaging Spectrograph on the Hubble Space Telescope we investigate B abundances in the Hyades F stars to look for a potential B dip using the B I resonance line at 2496.8 Å. The light elements, Li, Be, and B, are destroyed inside stars at increasingly hotter temperatures: 2.5, 3.5, and 5 $\times 10^6$ K respectively. Consequently, these elements survive to increasingly greater depths in a star and their surface abundances indicate the depth and thoroughness of mixing in the star. We have (re)determined Li abundances/upper limits for 79 Hyades dwarfs, Be for 43 stars, and B in five stars. We find evidence for a small drop in the B abundance across the Li-Be dip. The B abundances for the four stars in the temperature range 6100 - 6730 K fit the B-Be correlation found previously by Boesgaard et al. Models of rotational mixing produce good agreement with the relative depletions of Be and B in the dip region. We have compared our nLTE B abundances for the three high B stars on either side of the Li-Be dip with those found by Duncan et al. for the two Hyades giants. This confirms the factor of 10 decline in the B abundance in the Hyades giants as predicted by dilution due to the deepening of the surface convection zone.

Subject headings: stars: abundances; stars: evolution; stars: late-type; stars: solar-type; open clusters and associations: general; open clusters and associations: individual (Hyades)

1. INTRODUCTION

The nuclei of the rare light elements, lithium, beryllium, and boron, are susceptible to destruction by fusion reactions in the interiors of cool main-sequence stars. Of this trio, Li is the most fragile, B the most robust. The destruction of Li by (p,α) type reactions occurs at a temperature of $\sim$2.5 x 10^6 K, while Be is destroyed at $\sim$3.5 x 10^6 K. Inasmuch as B is not destroyed until $\sim$5 x 10^6 K, it serves as a probe to even deeper layers inside stars. The determination of the degree of depletion of Li, Be, and B in stellar atmospheres serves as a monitor of internal stellar processes and kinematics. The surface content of these elements provides information about the redistribution of matter and the mixing patterns within a

[1]Based on observations made with the NASA/ESA Hubble Space Telescope, obtained at the Space Telescope Science Institute, which is operated by the Association of Universities for Research in Astronomy, Inc., under NASA contract NAS 5-26555. These observations are associated with program #HST-G0-12294.

star. Thus, spectroscopic studies of these three elements expose the otherwise hidden stellar interior.

The stars of an open star cluster provide a perfect laboratory to make observations of all three elements for this type of investigation because their stars have a common origin and a known age and metallicity. The abundances of Li, Be, and B that were present in the interstellar medium at the birth of the cluster are what all of the stars would have had *ab initio*. Since all the stars start with the same abundance of each light element, the present-day abundance of each then reveals the deficiency pattern as a function of stellar mass and thus supplies guidance on the internal mixing processes. For main sequence stars in a given cluster the effective temperature is a good surrogate for stellar mass.

The relatively nearby Hyades cluster is $\sim$7 x 10^8 yr old and has a metallicity of [Fe/H] = +0.13 $\pm$0.02 (Boesgaard 1989, Boesgaard & Friel 1990). Recent studies have similar results, e.g. Paulson et al. (2003) find +0.13 $\pm$0.01, and Maderak et al. (2013) find +0.13 $\pm$0.01. See also Dutra-Ferreira et al. (2016). The errors quoted correspond to the error in the mean. The abundances of Li in the main-sequence stars in the Hyades were first done by Herbig (1965) and Wallerstein et al. (1965). The fall-off of Li with temperature in the Hyades **G dwarfs** has been investigated in several subsequent papers including Duncan (1981), Cayrel et al. (1984), Soderblom et al. (1990), Thorburn et al. (1993). The **F dwarfs** in the Hyades were studied by Boesgaard & Tripicco (1986) who discovered large Li depletions in the mid-F dwarfs; those depletions are factors of 100 relative to stars only 200 K hotter and cooler. That data set of 20 stars was augmented by Boesgaard & Budge (1988) so that some 30 stars outlined the Hyades F star Li dip. This "chasm" in the Li abundance occurs in the temperature range 6400 - 6850 K. In hindsight we can see that there was a hint of this Li dip in the Hyades F dwarfs in upper limits found for Li in the Wallerstein et al. (1965) paper where they could measure only Li upper limits on their spectrographic plates.

Boesgaard & King (2002) completed an investigation of Be in 34 Hyades F and G dwarfs. They found the Be counterpart to the Li dip in the **F dwarfs**. There is no Be counterpart to the Li deficiencies in the **G dwarfs**; this had been first indicated in a study by Garcia Lopez et al. (1995) of Be in four cool Hyades dwarfs. The Be-dip in the Hyades F stars is not as deep as the Li dip; Be detections go down to a factor of 7 below the meteoritic value of 1.42 (Grevesse & Sauval 1998).

This Li-Be dip contradicts the predictions of standard stellar evolution theory. The surface convection zones (SCZ) in mid-F stars are far too shallow for light element depletion to occur through convective mixing alone. The standard theory ignores a number of conditions that could affect the light element abundances, such as rotation, diffusion, mass loss, turbulence, internal gravity waves, etc. These effects could result in additional mixing

below the SCZ. The more observational information we have for all three light elements, the better we will be able to understand the internal mixing processes and then build more sophisticated stellar evolution models.

Studies of Li abundances in clusters younger than the Hyades, such as Pleiades and α Per, found only a small, if any, dip in Li (Pilachowski et al. 1987, Boesgaard et al. 1988). The conclusion was that the Li reductions occurred after the stars were already on the main-sequence; it was not a pre-main sequence phenomenon.

Explanation for Li depletion was attributed to several causes. An excellent discussion of these various mechanisms is given in Stephens et al. (1997). Lithium (and other elements) could be carried away in mass loss through stellar wind mechanisms. Diffusion between the surface convective and the radiative zones of the star could reduce the surface abundance. Pinsonneault et al. (1989) investigated a rotating solar model and the effects on rotationally-induced mixing on Li and Be abundances. Zahn (1992) found that such mixing could be applied as an explanation for the sudden depletion of Li over the narrow range of dip stars. Using Zahn's models, Charbonnel et al. (1994) were able to very closely model the cool, "red" side of the dip for both Li and Be abundances. Deliyannis & Pinsonneault (1997) correlated Li and Be depletions to rotationally induced mixing as an explanation of the dip. (Balachandran (1995) showed that post-turnoff stars in M 67 show Li deficiencies, not the initial Li abundances of the cluster. Thus the Li had been destroyed on the main sequence rather than disappearing by nondestructive diffusion which would have brought up Li atoms from the radiative zone.)

Deliyannis et al. (1998) and Boesgaard et al. (2001) have shown that Li and Be abundances are correlated in F field stars on the cool side of the Li-Be dip ($T_{\rm eff}$ = 5900 - 6650 K). Boesgaard & King (2002) discovered that the Hyades stars in this same temperature range show the same correlation between A(Li) and A(Be). The slope – in both Hyades and field stars – of this remarkable logarithmic relationship is +0.36. Boesgaard et al. (2004b) found a similar correlation in the six open clusters and additional field stars. Their figures 8b and 10 show this correlation for the field and cluster stars in the range $T_{\rm eff}$ = 6300 - 6650 K which has a slope of +0.43 $\pm$0.04. Their figures 8a and 9 cover $T_{\rm eff}$ = 5900 - 6650 K with a slope of 0.38 $\pm$0.03 that is well-matched by the predictions of the rotation models of Deliyannis & Pinsonneault (1993, 1997) and Charbonnel et al. (1994).

From the observations of the Li-Be dip in F stars in the Hyades and other clusters, the question naturally arises: "Is there also a dip in B in the Hyades F stars?" This is quite possible as deficiencies of B have been found in F field stars. Boesgaard et al. (2005) discovered a a correlation between Be and B from HST/STIS Cycle 10 observations of 18 stars of which 13 were very depleted in Be. From the B observations in that work they

discovered that the F5 V star, HR 107, is deficient in all three elements. It is deficient in Li by a factor of at least 650, in Be by 25 or more, and in B by 10. Here we report on the abundance of all three light elements in the Hyades cluster F dwarf stars. The well-studied Hyades cluster provides the best venue for this investigation, but the results are important for our understanding of field stars as well.

2. OBSERVATIONS AND DATA REDUCTION

2.1. HST Boron Observations

Observations with the STIS instrument on the *Hubble Space Telescope* were made of vB 14 on 2003 September 9 to determine the B abundance as part of a program to look at B through the Li-Be dip in the Hyades. The four other stars in that program were not observed by the time that STIS died. After the servicing mission (SM4) restored STIS to life, we received an additional four orbits to observe B in two stars in the Li-Be dip region of the Hyades: vB 13 and vB 37. We were able to supplement these observations with spectra covering the B region of two Hyades dwarf stars in the HST archive. The log of these observations is given in Table 1 and the location of the five stars in the HR diagram is shown in Figure 1. The values for luminosity and effective temperature are taken from de Bruijne et al. (2001).

The data reduction was provided by the standard HST/STIS and GHRS pipelines. Figure 2 shows a six Å region of the ultraviolet spectra of two of the stars, vB 14 and vB 65, near the B I line at λ2496. These two stars differ in temperature by almost 900 K which affects the line strength of the B I line as well as the blending lines. One can see significant line-crowding in this region.

2.2. Lithium and Beryllium Observations with Keck/HIRES

Observations of 17 Hyades stars were made at Keck I with HIRES (Vogt et al. 1994) on the nights of 1999 January 17 and 18 UT. These spectra covered the range of 5700 to 8100 Å (with some inter-order gaps) and have a spectral resolution of ∼48,000 and 24μ pixels. On each night 15 quartz flat field exposures were obtained along with 15 bias frames. Comparison spectra of Th-Ar were taken at the beginning and the end of each night. Three additional spectra were kindly obtained for us by G.H. Herbig on the night of 2005 November 23; these were taken with the updated version of HIRES with the mosaic CCDs with 15μ pixels. Quartz, dark, and Th-Ar frames were also taken. The log of the observations of all

20 stars is given in Table 2. The positions of these stars in the HR diagram are shown in Figure 3.

The data reduction was done with IRAF[2] and followed standard procedures with bias subtraction, flat field corrections, order extraction, wavelength calibration, continuum fitting. Samples of these spectra are shown in Figure 4. The spectrum of the coolest of the three stars shows considerable depletion of Li while the neighboring Fe I lines (6703, 6705 and 6710 Å) are increasing in strength with decreasing temperature.

Most of the observations used here for Be were originally reported by Boesgaard & King (2002). We obtained spectra of 10 additional Hyades stars for Be with Keck I and the upgraded HIRES with the new high-sensitivity UV chip with 15μ pixels. Those observations are also listed in Table 2. The quartz flat-field exposures needed for the Be region were 50 s to achieve the proper signal that far in the UV. We took seven quartz frames at 50 s, seven at 3 s and seven at 1 s as needed for the three CCDs. In addition we took 11 bias frames and Th-Ar exposures at both the beginning and the end of the night. The positions in the HR diagram of the new stars as well as the stars observed earlier for Be are shown in Figure 5. Data reduction was done with the MAKEE pipeline and with IRAF. Examples of two those new spectra covering a region of 2.2 Å are shown in Figure 6 where the positions of the two resonance lines of Be II are marked.

3. STELLAR PARAMETER DETERMINATION

de Bruijne et al. (2001) have done a detailed study of the parameters for the Hyades stars from the Hipparcos results for 92 high-fidelity stars. They have used two calibrations in converting $(B-V)$ and M_V to log $T_{\rm eff}$ and log $(L/L_\odot)$.

The recalibration of the Hipparcos data by van Leeuwen (2007) give the distance to the Hyades of 46.45 ±0.50 pc. The earlier distance from Perryman et al. (1998) was 46.34 ±0.27 pc. We conclude that there is no justification for changing the parameters of de Bruijne et al. (2001) based on the new calibration of van Leeuwen (2007).

We have determined values for the microturbulent velocity, ξ, from the empirical relationship of Edvardsson et al. (1993) with dependencies on $T_{\rm eff}$ and log g. Values for stellar masses were determined by interpolating our derived $T_{\rm eff}$ along the isochrones in Pinson-

[2]IRAF is distributed by the National Optical Astronomy Observatories, which are operated by The Association of Universities for Research in Astronomy, Inc., under cooperative agreement with the National Science Foundation.

neault et al. 2004, which are specific to the Hyades. We use values of v sin i primarily from Mermilliod et al. (2009), but also from Paulson et al. (2003), Reiners & Schmidt (2003), and Kraft (1965) for the Hyades. We adopt [Fe/H] = 0.13, as discussed in the introduction.

In Table 3 we list the values we use for $T_{\rm eff}$, log g, stellar mass, ξ, v sin i, and the depth of the surface convection (SCZ) as a fractional radius. The star names are listed as van Buren, HD and HIP numbers. For the depth of the SCZ of these stars we have used the models detailed in Table 2 of van Saders & Pinsonneault (2012). We have interpolated among the mass, He abundance, age, and metallicity. We calculated the mass of our Hyades sample using temperature values from Hipparcos data (de Bruijne 2001) and interpolating in Table 2 from Pinsonneault et al. (2004) which is specific to the Hyades. We select a He abundance value of 0.271 ±0.006 from Pinsonneault et al. (2003), and use our [Fe/H] value of 0.13. We select 650 Myr as the Hyades age as a compromise between the commonly used value of 625 Myr (±50 My) from Perryman et al. (1998), and the slightly older value of 750 Myr (±100 My) from Brandt and Huang (2015). In the case where one of the parameters lies outside of the van Saders & Pinsonneault table coverage, we extrapolated using the two nearest table entries. If two or more parameters were outside of the range of the table, we instead interpolated for the SCZ depth directly, using $T_{\rm eff}$ and depths from similar stars in our Hyades sample.

4. ABUNDANCE DETERMINATIONS

Boron abundances were found by spectrum synthesis using the program MOOG(2011 version)[3] (Sneden 1973). The line list in the B I region is from Duncan et al. (1998) with small modifications as in Boesgaard et al. (2005). We excluded lines from Duncan's original line list that extremely negative log gf values (<-5) and those with very high excitation potentials (>6 ev). We relied on the synthesis around the 2496.8Å line. (The wavelengths given are air wavelengths.) We also attempted to include synthesis around the 2497.7 Å region, but found that blending with the strong iron and cobalt features in the region prevented any meaningful evaluation of B abundance from that line.

In the synthesis we adopted [Fe/H] = 0.13 as discussed in the introduction. In the models all elements, other than B, are increased by that same amount. This is a valid assumption within the 3 Å range surrounding the fitted region (2495.500-2498.500 Å) for several reasons. The abundance of "iron-peak" elements (V, Cr, Mn, Co, Ni) plus Al, track with that of [Fe/H] (Carrera & Pancino 2011), and the majority of lines in the full list from

[3]http://www.as.utexas.edu/∼chris/moog.html

Duncan et al. (1998) (135/185) are from these elements. Of the other line sources, Ti and Sc are (possibly) slightly depleted with respect to iron (-0.06 and -0.02), respectively, Carrera & Pancino 2011), however this minor difference, combined with the relative lack of lines (7/185) does not contribute to a measurable difference in the synthesis. The remaining line sources consist of N, F, P, Cl, and Ge and heavier elements with insufficiently determined abundances to make accurate adjustments.

Line broadening was calculated by the MOOG synth driver using the "r" option, which combines v *sin* i, macroturbulence, and generic "Gaussian" factors. We used the values of v *sin* i from Table 3 but had no direct measurement of macroturbulence or of the Gaussian factors (which would include sources such as instrumental broadening). These two factors were fit as free parameters during the chi-squared reduction process. The best indicator of these two factors was the prominent Fe II feature at 2497.3Å, although other features were also considered.

We determined our synthetic solution using a two-step chi-squared minimization technique. Initially, MOOG parameters for line broadening and wavelength and (normalized) flux offset and scaling, were adjusted manually to minimize the chi-squared statistic. The window from 2496.0 to 2497.5 Å, excluding the area of the 2496.8Å B line was used for this first iteration. Note that the B line width varies with the line broadening of a particular star. For stars with significant broadening, like vB 13, the region excluded in the first step is approximately 0.6Å wide (2496.5-2497.1Å). For lines with lesser broadening (eg. vB 62), the excluded range is slightly less than 0.5Å. The second step determined the B abundance which best matches the observed spectra by minimizing the chi-squared statistic for the region of the B line; the previously "excluded" region. The final B abundance corresponds to the abundance which has the lowest chi-squared value for the points within the B line.

We show the synthesized B spectra in Figure 7 for vB 14, on the hot side of the Li-Be dip and vB 62 on the cool side of the dip. The LTE values for A(B) are 2.50 and 2.51, respectively. In Figure 8 are the syntheses for two stars in the Li-Be dip: vB 13 and vB 37 at 2.15 and 2.05 respectively

Boron abundances are subject to non-local thermodynamic equilibrium effects, and we have adjusted our abundance measures, as recommended by Kiselman & Carlsson (1996). Both uncorrected (LTE assumed) and nLTE abundances are given in Table 4. When corrected for nLTE effects, the values for A(B)n for vB 14 and vB 62 are 2.73 and 2.55. The two stars in the Li-Be dip have A(B)n of 2.32 and 2.24 respectively.

Errors for our B determinations due to the uncertainties in the stellar parameters are given in Table 5. Error values were obtained by altering a single model parameter by the

listed amount, and re-running the complete spectral synthesis in MOOG to determine the resulting change in abundance. The total uncertainty listed is the square root of the sum of the squares of the three parameters. Two of us of us did the B synthesis independently for 3 of the stars; there was a mean difference of 0.03 dex.

We have determined Li abundances for all 20 stars by spectrum synthesis using the synth driver in MOOG. The synthesis for Li is less complex than for B and there are far fewer lines. We may have small adjustments in wavelength and in Gaussian smoothing to make. This can be seen in Figure 9 where the fit over the 8 Å region is excellent. The Li abundances are also given in Table 4. In addition, we have modified published values (from Boesgaard & Budge 1988, Boesgaard & Tripicco 1986, Cayrel et al. 1984 and Thorburn et al. 1993) for A(Li) in the other stars to reflect the parameters in Table 3 from de Bruijne et al. (2001). Fortunately, A(Li) is dependent only on the model temperature. We have found that there is no difference in A(Li) with log = 4.0 vs. 4.5. There is no difference with [Fe/H] = +0.1, 0.0, and even −1.0. The difference in temperature of ±100 K is ±0.08 dex in A(Li). There are four stars for which we have new observations with A(Li) determined here with Li synthesis and for which we redetermined A(Li) with the equivalent widths from Boesgaard & Tripicco (1986) and Boesgaard & Budge (1988) using the blends driver in MOOG. The stars are vB 14, 37, 62, 65 and the ΔA(Li) values are 0.01, 0.00, 0.06 and 0.00, respectively, for "blends" minus "synth." Our revised values for A(Li) are given in Table 4.

Takeda et al. (2013) have determined abundances for Li, C, and O in the Hyades F and G dwarfs using spectral synthesis. They also used the de Bruijne et al. (2001) stellar parameters derived from *Hipparcos* data. We have 12 stars in common with them for which we both found A(Li) from spectral synthesis, excluding an additional two for which we both found upper limits on Li. The mean difference in our A(Li) minus theirs is −0.06 ±0.09. If we exclude the two most discrepant stars, vB 26 and 42, among the very coolest in each of our samples and thus the weakest Li lines, the mean difference is −0.03 ±0.07. This is excellent agreement.

Beryllium abundances for 34 Hyades F and G dwarfs were done by Boesgaard & King (2002) using spectrum synthesis; they were later reanalyzed in Boesgaard et al. (2004a) using the later version of MOOG which included Kurucz's UV opacity edges, the metal bound-free opacity contributions adapted from the ATLAS model atmosphere code (e.g. Kurucz et al. (2011 and references therein.) We have now readjusted those abundances to reflect the parameters that we have used here; Be abundances are sensitive to both $T_{\rm eff}$ and *log* g. We have synthesized the newly obtained Be spectra, but were unable to get a reasonable fit for the coolest star, vB 178 at 5235 K. The Be abundances for 43 stars are also given in Table 4.

5. RESULTS

5.1. B in the Li-Be Dip

Figure 10 shows the Hyades Li abundances as A(Li) as a function of $T_{\rm eff}$ for both Li detections and upper limits.[4] The drop in Li in the temperature range 6350 to 6800 K is the Li dip where the values for A(Li) span nearly two orders of magnitude. The decline in A(Li) with decreasing temperatures begins near 6000 K. Superimposed on this plot are the nLTE B abundances, A(B)n, on the same vertical scale as the Li abundances. Both A(Li) and A(B) are plotted with relative to their respective meteoritic abundances. There are two stars, vB 13 and vB 37, with B abundances that are in the Li-dip region. Both stars appear to be depleted in B.

In Figure 11[5] we show the Hyades B and Be abundances on the same vertical scale as in Figure 10. They are also plotted relative to their respective meteoritic abundances. The Be dip is less pronounced than the Li dip, but covers almost an order of magnitude. Although there is a decline in A(Li) in G dwarf stars cooler than 6000 K, there is no such decline in A(Be). See Figure 10. The two stars in the Li dip, vB 13 and vB 37, appear to be depleted in B with respect to Be as well as with respect to Li.

The best mechanism for the decreased values for Li and Be on the cool side of the Li-Be dip appears to be rotationally-induced mixing at the base of the SCZ, which mixes Li and Be nuclei down to the region of critical temperatures for destruction as discussed in the Introduction (§ I).

Figure 12 plots the rotational velocities as v *sin* i from Table 3 against their $T_{\rm eff}$ values for our Hyades sample. Böhm-Vitense (2004) characterized the transition from the most rapidly rotating stars, at $T_{\rm eff}$ around 7000 K and above, to the slower rotators at 6000 K and below, as a "step" function. Even with the uncertainty due to *sin* i, our data show a steep slope over the temperature region of the Li-Be dip as first noted by Boesgaard (1987). The cooler stars have apparently spun down to v *sin* i values of $\sim$5 km s^{-1} typically, by 6100 K.

Over this same range in temperature, the surface convection zone is deepening as shown in Figure 13 from the data in Table 3. The SCZ is extremely shallow in stars hotter than

[4]Stars that appear in Table 4 but are excluded from this figure are vB 77 and vB 78 with membership probabilities of 1% and 21% according to Hanson (1975). We exclude vB 143 and concur with Thorburn et al. (1993) that it is not a Hyades member. Also excluded is vB 124 which is a quadruple system of two SB2 pairs (Griffin et al. 1985, Turner et al. 1986, Tomkin & Griffin 2007).

∼7000 K and by ∼5500 K it extends over the top 30% of the stellar radius. Both the apparent "spinning down" of stars around the dip and the increase of the depth of the convection zone provide additional information that the depletion of the light elements in this regime occurs by rotational-mixing mechanisms. Our measurement of a smaller B depletion over that of Be and Li in the "dip" continues to conform best with models which incorporate rotationally induced mixing. We note that in four Hyades Am stars hotter than 7500 K Burkhart & Coupry (1989) found no Li depletion.

Detailed mathematical models of the hydrodynamic processes in the "dip" stars by Garaud & Bodenheimer (2010) used "gyroscopic pumping" to model deep mixing, down the rotation axis, and into regions where all three light elements can burn. Their Figure 11 shows a diagram of these flows. While the process model accounts for Li and Be, it does not specifically deal with B. However, even without access to a working simulation, their models appear to predict a lesser, but non-zero depletion of B in the dip stars. Specifically we note that, due to the deeper radius of B burning and the linear (log) scaling of the circulation timescale to that depth, the timescale for B depletion will be longer than those of Li and Be. See their Figure 12. Although their model of gyroscopic pumping reproduces the cool side of the depletion "dip" well, it must rely on (outward) diffusion in order to replenish (overly) depleted Li and Be (and we assume B) on the hot side of the dip. However, they produce a reasonable model for surface replenishment through a diffusion from the radiative to the convective zone, which brings the models well in line of the observations of both the Li and Be non-depletion on the hot side of the dip.

5.2. The Be-B Correlation

Of the three elements, Li, Be, and B, it is Li that is the most fragile; the nuclear reactions that destroy Li occur at temperatures as cool as ∼2.5 x 10^6 K. The nuclei of Be atoms can survive at deeper depths where the temperatures are near 3.5 x 10^6 K. The Li observed in the stellar photosphere may be severely depleted while the surface Be is unaffected or mildly depleted. A correlation between the abundance (and depletions) of Li and Be in late F- and early G-dwarf field stars was found by Deliyannis et al. (1998) and Boesgaard et al. (2001).

This correlation of Li and Be depletions was well-matched by rotationally-induced mixing of Deliyannis and Pinsonneault (1993, 1997) and Charbonnel et al. (1994). This was further studied by Boesgaard et al. (2004b) in field and cluster stars. The temperature range where the depletions are correlated corresponds to the cool side of the Li-Be dip from the bottom of the Li dip near 6500 K to the Li-peak around 6000 K. The stars observed for both Li and Be were 46 field stars and 42 stars from five open clusters. In particular,

their Figure 12 shows the *data* as a line from the least-squares fit of the observed A(Li) and A(Be) and the model predictions for three different ages (0.1, 1.7, and 4.0 Gyr) and two different initial rotational velocities (10 and 30 km s^{-1}). The data and the theory are well-matched; the theory is slightly offset and is plotted and A(Be) −0.14. As the stars age they march down that line with less and less Li and Be with Li decreasing faster than Be. The inclusion of stars with different ages revealed the same correlation. These are slow, but apparently simultaneous depletions. The metallicity of the stars is not really relevant until [Fe/H] <-0.25.

This work led Boesgaard et al. (2005) to search for B in F and G dwarf stars that were depleted in Be. Such stars would presumably not have detectable Li as indicated by the Li-Be correlation. They included five stars with "normal" Li and Be abundances. Inasmuch as B nuclei can survive to deeper depths where the temperatures are near 5 x 10^6 K, they studied B in stars that were severely Be-depleted. They found a correlation between the Be and B (as corrected for nLTE effects) depletions. As A(Be) goes from 1.4 to −0.5, A(B) declines from 2.4 to 2.0. Boron is the most robust of the three light elements. The slope of A(Be) versus A(B) was 0.22 for the range in $T_{\rm eff}$ from T = 6100 − 6730 K. We have overplotted our four cool Hyades stars on their results for the 14 field stars in Figure 14. The Hyades stars match the correlation field stars very well. The two Hyades stars in the Li-Be dip with depletions in both Be and B, vB 13 and vB 37, highlight the reality of the B depletions in the Hyades. As stars age they deplete both Be and B as was found for Li and Be.

In Boesgaard et al. (2004b) we showed how well theory which includes mixing-enhanced-by-rotation can match the observed plots of A(Li) vs. A(Be) in the temperature range of the Li-Be dip. With our new data, we present a matching theory for A(Be) vs. A(B) for the observations in Figure 14. To do this, we have updated our mixing calculations to include ^{10}B and ^{11}B, with an isotopic ratio of $n(^{10}{\rm B})/n(^{11}{\rm B}) = 0.247$ (Lodders 2003) and an initial abundance A(B) equal to the proto-solar value of 2.6. Our models track the dominant $^{10}{\rm B}(p,\alpha)^7{\rm Be}$ and $^{11}{\rm B}(p,\alpha)^8{\rm Be}$ reactions, with temperature-dependent rates from Caughlan & Fowler (1988) and updated astrophysical S(0)s from the NACRE-II compilation (Xu et al. 2013). With these additions, we computed mixing models with masses in the range of 1.15–1.45$M_\odot$, and initial angular momenta log(J) = 50.5 (fast), 50.1 (medium), and 49.7 (slow), where the units of J are g cm^{-2} s^{-1}. The corresponding values of rotational velocities are dependent on age, mass etc., but at 700 Myr at 1.25 $M_\odot$ (near the center of the Li-Be-B dip) they are approximately 15.7, 13.1 and 8.5 km s^{-1}.

Our mixing models are compared to the data in Figure 15. The colored lines show our predicted A(Be) vs. A(B) at 2 Gyr. These abundance tracks overlap one another and share

the same approximate slope, demonstrating that the predicted ratio of Be to B depletion is constant regardless of mass, age, and initial rotation conditions. Our predicted correlation between Be and B depletion nicely matches the A(Be) vs. A(B) trend revealed by the data, supporting a mixing origin for the abundance ratios of these two elements. We note that our models over-predict the B abundance of the Hyades members by about ~ 0.1 dex, perhaps reflecting inaccuracies in the B nuclear cross sections, missing physics in our models, or a true initial Hyades B abundance lower by ~ 0.1 dex. (This amount of offset is like that of the A(Li) vs. A(Be) described in the second paragraph above.) However, the relative B abundance difference of $\sim 0.15-0.2$ dex between the lower mass stars at A(Be)$\sim$1.1 and the higher mass stars at A(Be)$\sim$0.6 is accurately predicted. The black star indicates the highest elemental depletion predicted by 700 Myr, showing that sufficient B depletion by mixing is predicted at the age of the Hyades, and that the ratio of Be to B depletion is constant with age. The good agreement between our predictions and these B abundances bolsters the success of rotational mixing as an explanation for the cool side of the Li-Be-B dip.

We stress that the consistency of the Be to B depletion ratio between the field stars, which presumably have a variety of ages, and the Hyades is very striking, as is the constancy of the Li to Be depletion ratio, that we have found repeatedly in our previous works. This Li-Be-B depletion correlation dictates very fundamental constraints on how stellar interiors mix. The agreement with the present models of B/Be depletion and our earlier similar models of Li/Be depletion (Deliyannis et al. 1997, 1998) suggests that a star doesn't care how long it takes to reach a particular Be depletion, or how fast the star was rotating previously: when a particular Be depletion is achieved, remarkably, unambiguous corresponding depletions of B and Li are also achieved.

5.3. Comparison of B in the Hyades Dwarfs with B in the Hyades Giants

The light-element abundances have provided many tests of stellar evolution theory. Iben (1965, 1967) described the principle that Li, Be, and B would be diluted as the outer convection zone expanded and deepened during the star's evolution from the main-sequence to the giant branch. The small layer of surface Li would be diluted by Li-free matter bf below as the convection zone deepened, resulting in a major effect on the Li abundance visible on the surface of giant stars. The somewhat larger outer layer of Be would suffer a smaller dilution effect. These predictions were initially tested for Li by Herbig & Wolff (1966) and for Be by Boesgaard & Chesley (1976). Similarly, the even greater reserves of B would be even less diluted.

Duncan et al. (1998) studied B abundances in two Hyades giants as well as one dwarf,

vB 14. They determined that the two giants were deficient in B relative to the dwarf by a factor of ∼10. That amount of decrease in B was a good match for Iben's model predictions. Other models predict even more B depletion in red giants. Sackmann & Boothroyd (1999) show that the extra-deep circulation that creates ^{7}Li, if long-lived, would destroy all Be and B. The Hyades red giants show no excess Li, so that process is not relevant here. In addition, their calculations show that if a star spends more than 10,000 years on the red giant branch both Be and B plummet. (See their Figure 7.) The models of Lagarde et al. (2012) include extra-mixing from rotation and thermohaline instability which would circulate Li, Be, B down to deeper layers. There more B atoms would be destroyed, beyond the factor of 10 from dilution alone. However, for the Hyades giants the observations show that B is diluted as in Iben's models, but not destroyed.

We have B abundances for one star on the hot side of the Li-Be-B dip and two on the cool side. Presumably these three stars contain the initial, undepleted B in the Hyades. The mean value is A(B)n = 2.54 ±0.12 consistent with the solar/solar system B abundance. The value for these three Hyades dwarfs is similar to that found by Duncan et al. (1998) and confirms the conclusions of that paper.

6. SUMMARY AND CONCLUSIONS

The dramatic drop in Li and Be abundances in the mid-F dwarfs has prompted our study of the B abundance in the Li-Be dip. We obtained spectra of 5 Hyades stars with HST to find B abundances from the B I line at 2497 Å. In addition we have made observations of Li in 20 stars with Keck I and HIRES for a total of 79 stars with Li abundances in the Hyades. We supplemented the 33 stars already observed with Keck for Be by Boesgaard & King (2002) with 10 new one for a total of 43 Be abundances.

We used the Hipparcos parameters determined for the Hyades stars by de Bruijne et al. (2001) and found abundances by spectrum synthesis for all three elements. We have produced new plots of the light-element abundances with temperature, normalizing all the previous results to the new parameters.

In our overplots of the B-temperature profile (scaled to the Li and to the Be results) we find evidence for a drop in B abundance across the Li-Be dip. In the temperature region of approximately 6400 – 6800 K, A(Li) drops by a factor of more than 100, while A(Be) drops by a factor of 10. The drop in A(B)n is about a factor of 2.5. We can now refer to the Hyades Li-Be-B dip.

We also find that A(Be) and A(B)n in the four cool Hyades stars conform to the B-Be

correlation found for field stars in that temperature range by Boesgaard et al. (2005). That logarithmic relationship has a slope of +0.22 as A(Be) is depleted more than A(B)n. There is a similar correlation between A(Li) and A(Be) with a slope of +0.36 where Li is more depleted than Be. Both relationships show plausible zero-point shifts at the 0.1 dex level which are suggested, but not required by the data.

The three of our non-dip stars appear to be undepleted B. The mean of A(B)n is 2.54 ±0.12 compared to the solar values of 2.60. The Hyades giants will have undergone dilution of the three light elements due to the expansion of the surface convection zone. We compared this main-sequence "initial" B abundances with that found in two Hyades giants by Duncan et al. (1998). The B in the giants has been diluted by a factor of ∼10, in agreement with the predictions of standard evolution models by Iben (1965, 1967).

We are grateful to the Keck Observatory support astronomers for their knowledgeable assistance during our observing runs. Special thanks to the late Dr. George H. Herbig for obtaining HIRES spectra of three Hyades stars for which there were HST B observations. We would like to thank Drs. Jeffrey Rich and C. J. Ma for their assistance in data reduction. We are also grateful to students Jennifer Beard and Edward Lever for their assistance. This work has been supported by HST-GO-09886 and HST-GO-12294, and NSF grants AST-00-97955 and AST-05-05899.

REFERENCES

Balachandran, S. 1995, ApJ, 446, 203

Boesgaard, A.M. 1987, PASP, 99, 1067

Boesgaard, A.M. 1989, ApJ, 336, 798

Boesgaard, A.M., Armengaud, E. & King, J.R. 2004a, ApJ, 605, 864

Boesgaard, A.M., Armengaud, E., King, J.R., Deliyannis, C.P. & Stephens, A. 2004b, ApJ, 613, 1202

Boesgaard, A.M. & Budge 1988, ApJ, 332, 410

Boesgaard, A.M., Budge, K.G. & Ramsay, M.E. 1988, ApJ, 327, 389

Boesgaard, A.M. & Chesley, S.E. 1976, ApJ, 210, 475

Boesgaard, A.M., Deliyannis, C.P., King, J. K. & Stephens, A. 2001, ApJ, 553, 754

Boesgaard, A.M. & Friel, E.D. 1990, ApJ, 351, 467

Boesgaard, A.M. & King, J.R. 2002, ApJ, 565, 587

Boesgaard, A.M., Deliyannis, C.P. & Steinhauer, A. 2005, ApJ, 621, 991

Boesgaard, A.M. & Tripicco, M.J. 1986, ApJL, 302, L49

Böhm-Vitense, E. 2004, AJ, 128, 2435

Brandt, T.D. & Huang, C.X. 2015 ApJ, 807, 58

Burkhart, C. & Coupry, M.F. 1989, A&A, 220, 197

Carrera, R & Pancinoo, E. 2011 A&A, 535, 30

Caughlan, G.R & Fowler, W.A. 1988, ADNDT, 40, 283

Cayrel, R., Cayrel de Strobel, G., Campbell, B., & Däppen, W. 1984, ApJ 283, 205

Charbonnel, C., Vauclair, S., Maeder, A., Meynet, G., & Shaller, G. 1994, A&A, 283, 155

de Bruijne, J.H.J., Hoogerwerf, R. & de Zeeuw, P.T. 2001, A&A, 367, 111

Deliyannis, C.P. & Pinsonneault, M.H. 1993, in ASPCS 40, IAU Colloq. 137, p. 174

Deliyannis, C.P. & Pinsonneault, M.H. 1997, ApJ, 488, 836

Deliyannis, C. P., Boesgaard, A. M., Stephens, A., King, J. R., Vogt, S. S. & Keane, M. 1998, ApJL, 498, L147

Duncan, D.K. 1981, ApJ, 248, 651

Duncan, D.K, Peterson, R., Thorburn, J. & Pinsonneault, M.H. 1998, ApJ, 499, 871

Dutra-Ferriera, L., Pasquini, L., Smiljanic, R., Porto de Mello, G.F. & Steffen, M. 2016, A&A, 585, 75D

Edvardsson, B., Andersen, J., Gustafsson, B., Lambert, D. L., Nissen, P. E. & Tomkin, J. 1993, A&A, 275, 101

Garaud, P. & Bodenheimer, P. 2010, ApJ, 719, 313

Garcia Lopez, R., Rebolo, R. & Perez de Taoro, M. 1995, A&A, 302, 184

Grevesse, N. & Sauval, A.J. 1998, Space Sci. Rev., 85, 161

Griffin, R.F., Gunn, J.E., Zimmerman, B.A. & Griffin, R.E.M. 1985, AJ, 90, 609

Hanson, R.B 1975, AJ, 80, 379

Herbig, G.H. 1965, ApJ, 141, 588

Herbig, G.H. & Wolff, R.J. 1966, AnAp, 29, 593

Iben, I. 1965, ApJ, 142, 1447

Iben, I. 1967, ApJ, 147, 624

Joner, M.D., Taylor, B.J., Laney, C.D. & van Wyk, F. 2006, AJ, 132, 1111

Kiselman, D. & Carlsson, M. 1996, A&A, 311, 680

Kraft, R. P. 1965, ApJ, 142, 681

Kurucz, R. 2011, CaJPh, 89, 417

Lagarde, N., Decressin, T., Charbonnel, C., Eggenburger, P., Ekstrom, S. & Palacios, A. 2012, A&A, 543, 108

Lodders, K. 2003, ApJ, 591, 1220

Maderak, R.M., Deliyannis, C.P. King, J.R. & Cummings, J.D. 2013, AJ, 146, 143

Mermilliod, J.-C., Mayor, M. & Udry, S. 2009, A&A, 498, 949

Paulson, D.B., Sneden, C. & Cochran, W.D. 2003, AJ, 125, 3185

Perryman, M. A. C., Brown, A. G. A., Lebreton, Y., Gomez, A., Turon, C., Cayrel de Strobel, G., Mermilliod, J. C., Robichon, N., Kovalevsky, J. & Crifo, F. 1998 A&A, 331, 81

Pilachowski, C., Booth, J. & Hobbs, L.M. 1987, PASP, 99, 1288

Pinsonneault, M.H., Kawaler, S.D., Sofia, S. & Demarque, P. 1989, ApJ, 338, 424

Pinsonneault, M.H., Terndrup, D.M., Hanson, R.B. & Stauffer, J.R. 2003, ApJ, 598, 588

Pinsonneault, M.H., Terndrup, D.M., Hanson, R.B. & Stauffer, J.R. 2004, ApJ, 600, 946

Reiners, A. & Schmidt, J.H.M.M. 2003, A&A, 412, 813

Sackmann, I.-J. & Boothroyd, A.I. 1999, ApJ, 510, 217

Soderblom, D. R., Oey, M. S., Johnson, D.R.H., & Stone, R. P. S. 1990, AJ, 99, 595

Stephens, A, Boesgaard, A.M., King, J.R., & Deliyannis, C.P. 1997, ApJ, 491, 339

Takeda, Y., Honda, S., Ohnishi, T., Ohkubo, M., Hirata, R. & Sadakane, K. 2013, PASJ, 65, 53

Thorburn, J., Hobbs, L.M., Deliyannis, C. P., & Pinsonneault, M.H. 1993, ApJ, 425, 150

Tomkin, J. & Griffin, R.F. 2007, Obs., 127, 87

Turner, D.G., Lyons, R.W. & Bolton, C.T. 1986, Obs., 106, 13

Upgren, A.R. & Weis, E.W. 1977, AJ, 82, 978

van Leeuwen, F. 2007, A&A, 474, 653

van Saders, J.L. & Pinsonneault, M.H. 2012, ApJ, 746, 16

Vogt, S. S. et al. 1994, Proc. SPIE, 2198, 362

Wallerstein, G., Herbig, G.H. & Conti, P. 1965, ApJ, 141, 610

Xu, Y., Takahashi, K, Goriely, S. Arnould, M., Ohta, M. & Utsunomiya, H. 2013, Nuc. Phys. A, 918, 61

Zahn, J.-P. 1992, A&A, 265. 115

This preprint was prepared with the AAS LaTeX macros v5.2.

Table 1. Log of the HST Observations

vB	HD	HIP	Spectral Type	V	B-V	Date (UT)	Exp (sec)	Instrument
13	26345	19504	F6V	6.576	0.429	2011 Sep 16	9752	STIS/E230M
14	26462	19544	F4V	5.699	0.327	2003 Sep 20	1804	STIS/E230M
37	27561	20357	F5V	6.578	0.421	2011 Sep 16	6750	STIS/E230M
62	28033	20712	F8V	7.35	0.51	2003 Mar 15	2358	STIS/E230H
65	28205	20815	F8V	7.404	0.535	1995 Sep 12	7072	GHRS/270M

Table 2. Log of the Keck/HIRES Li and Be Observations

vB	HD	HIP	Spectral Type	V	B-V	Date (UT)	Exp (min)	S/N Li I or Be II
Li Observations								
13	26345	19504	F6V	6.58	0.429	2012 Jan 07	3	440
14	26462	19554	F4V	5.71	0.327	2005 Nov 23	0.5	499
15	26736	19793	G3V	8.09	0.658	1999 Jan 17	10	644
17	26756	19781	G5V	9.16	0.696	1999 Jan 18	18	820
18	26767	19786	G0V	8.06	0.638	1999 Jan 18	12	721
21	284253	19934	G5V	9.11	0.816	1999 Jan 18	15	586
26	27250	20130	G5V	8.63	0.743	1999 Jan 17	15	612
27	27282	20146	G8V	8.46	0.715	1999 Jan 17	12	628
31	27406	20237	G0V	7.47	0.566	1999 Jan 18	6	729
37	27561	20357	F5V	6.58	0.421	2012 Jan 07	3	440
42	27732	20480	G5V	8.85	0.759	1999 Jan 17	20	651
62	28033	20712	F8V	7.35	0.051	2005 Nov 23	1.5	432
64	28099	20741	G6V	8.12	0.657	1999 Jan 18	9	719
65	28205	20815	F8V	7.42	0.535	1999 Jan 17	5	669
73	28344	20899	G2V	7.85	0.609	1999 Jan 18	7	718
87	28593	21099	G8V	8.58	0.743	1999 Jan 17	15	658
92	28805	···	G8V	8.66	0.741	1999 Jan 17	15	647
93	28878	···	G5V	9.39	0.883	1999 Jan 18	20	633
97	28992	21317	G1V	7.94	0.634	1999 Jan 18	7	661
113	30311	22221	F5V	7.26	0.549	1999 Jan 17	5	683
121	30738	22524	F8V	7.27	0.48	2005 Nov 23	2	510
187	32347	23498	K0V	8.99	0.761	1999 Jan 18	15	630
Be Observations								
1	20430	15304	F8V	7.37	0.567	2014 Dec 27	8.3	80
2	20439	15310	G0V	7.75	0.617	2014 Dec 27	10	108
11	26051	19261	F3V	6.06	0.397	2014 Dec 27	1.7	105
18	26767	19786	G0V	8.06	0.638	2014 Dec 27	10.5	109
40	27691	20440	G0V	7.17	0.518	2014 Dec 27	5	111
49	27835	···	G0V	8.20	0.605	2014 Dec 27	10.8	98

Table 2—Continued

vB	HD	HIP	Spectral Type	V	B-V	Date (UT)	Exp (min)	S/N Li I or Be II
52	27859	20577	G2V	7.79	0.599	2014 Dec 27	10	112
73	28344	20899	G2V	7.85	0.609	2014 Dec 27	10	113
118	30589	22422	F8V	7.74	0.578	2014 Dec 27	10	130
178	28258	20850	G5V	9.08	0.839	2014 Dec 27	25	79

Table 3. Stellar Parameters

vB	HD[b]	Hip	B-V[a] (Hip)	$T_{\rm eff}$ (K)	log g	Mass ($M_\odot$)	ξ (km s^{-1})	v *sin* i (km s^{-1})	SCZ base
1	20430	15304	0.567	6079	4.446	1.19	1.38	5.5	0.766
2	20439	15310	0.617	5894	4.481	1.13	1.19	6.4	0.737
4	+23 465	16529	0.844	5223	4.579	0.94	0.53	3.4	0.694
6	24357	18170	0.354	7000	4.299	1.56	2.31	65.8	0.978
8	25102	18658	0.417	6705	4.329	1.45	2.03	54.0	0.910
9	+19 641	18719	0.705	5598	4.534	1.03	0.88	4.3	0.711
10	25825	19148	0.593	5983	4.464	1.16	1.28	6.5	0.749
11	26051	19261	0.397	6795	4.316	1.48	2.13	25.0	0.931
13	26345	19504	0.427	6660	4.336	1.43	1.99	27.2	0.900
14	26462	19554	0.360	6971	4.301	1.54	2.29	8.0	0.971
15	26736	19793	0.693	5757	4.506	1.08	1.05	5.6	0.722
17	26756	19781	0.640	5640	4.526	1.04	0.93	5.0	0.714
18	26767	19786	0.657	5812	4.497	1.10	1.10	4.4	0.728
19	26784	19796	0.514	6291	4.403	1.28	1.61	15.9	0.813
20	26911	19877	0.400	6783	4.318	1.48	2.11	···	0.928
21	284253	19934	0.813	5297	4.572	0.95	0.59	3.9	0.697
26	27250	20130	0.745	5485	4.549	1.00	0.77	3.6	0.705
27	27282	20146	0.721	5553	4.541	1.02	0.84	5.0	0.708
31	27406	20237	0.560	6107	4.440	1.20	1.41	10.2	0.771
36	27534	20350	0.441	6598	4.345	1.40	1.93	65.9	0.886
37	27561	20357	0.412	6728	4.326	1.46	2.06	20.4	0.916
38	27628	20400	0.315	7188	4.290	1.62	2.47	25.0	1.000
39	27685	20441	0.677	5692	4.518	1.06	0.98	4.0	0.717
40	27691	20440	0.518	6275	4.406	1.27	1.59	12.2	0.809
42	27732	20480	0.758	5449	4.554	0.99	0.74	3.0	0.703
44	27731	20491	0.462	6507	4.361	1.37	1.84	47.6	0.866
46	27771	20492	0.855	5196	4.582	0.93	0.50	4.8	0.693
48	27808	20557	0.518	6275	4.406	1.27	1.59	13.3	0.809
49	27835	···	0.605	5934	4.474	1.14	1.23	2.8	0.742
51	27848	20567	0.450	6558	4.352	1.39	1.89	40.3	0.877

Table 3—Continued

vB	HD[b]	Hip	B-V[a] (Hip)	$T_{\rm eff}$ (K)	log g	Mass ($M_\odot$)	ξ (km s^{-1})	v *sin* i (km s^{-1})	SCZ base
52	27859	20577	0.599	5961	4.468	1.15	1.26	6.7	0.746
57	27991	20661	0.509	6310	4.399	1.29	1.63	16.3	0.818
59	28034	···	0.555	6122	4.437	1.21	1.43	7.1	0.774
61	28069	20693	0.509	6306	4.400	1.28	1.62	22.3	0.817
62	28033	20712	0.556	6118	4.438	1.21	1.43	4.8	0.774
63	28068	20719	0.651	5776	4.503	1.09	1.07	7.7	0.724
64	28099	20741	0.664	5735	4.510	1.07	1.03	5.8	0.721
65	28205	20815	0.537	6199	4.421	1.24	1.51	11.1	0.791
66	28237	20826	0.560	6107	4.440	1.20	1.41	10.2	0.771
69	28291	20890	0.741	5497	4.548	1.00	0.79	4.0	0.705
73	28344	20899	0.609	5924	4.475	1.14	1.22	7.6	0.741
76	283704	20949	0.766	5426	4.557	0.98	0.72	3.0	0.702
77	28394	20935	0.526	6242	4.412	1.26	1.56	20.1	0.802
78	28406	20948	0.451	6554	4.352	1.39	1.89	28.8	0.876
79	285773	20951	0.831	5254	4.576	0.94	0.55	3.9	0.695
81	28483	21008	0.470	6474	4.367	1.35	1.80	24.5	0.858
85	28568	21053	0.428	6656	4.337	1.43	1.99	54.0	0.899
86	28608	21066	0.472	6465	4.369	1.35	1.79	30.4	0.856
87	28593	21099	0.734	5516	4.545	1.01	0.80	4.9	0.706
90	28736	21152	0.420	6693	4.331	1.44	2.02	39.8	0.908
91	28783	···	0.880	5135	4.585	0.92	0.47	3.6	0.692
92	28805	···	0.755	5453	4.553	0.99	0.74	4.3	0.703
93	28878	···	0.897	5095	4.574	0.91	0.43	6.5	0.690
94	28911	21267	0.429	6651	4.337	1.43	1.98	40.0	0.898
96	285931	21280	0.840	5216	4.580	0.93	0.52	8.1	0.694
97	28992	21317	0.631	5844	4.491	1.11	1.14	7.6	0.731
99	29159	···	0.867	5165	4.585	0.92	0.47	3.0	0.692
101	29225	21474	0.442	6593	4.346	1.40	1.92	41.0	0.885
102	29310	21543	0.597	5968	4.467	1.15	1.27	7.4	0.747
105	29419	21637	0.576	6045	4.452	1.18	1.35	4.3	0.760

Table 3—Continued

vB	HD[b]	Hip	B-V[a] (Hip)	$T_{\rm eff}$ (K)	log g	Mass ($M_\odot$)	ξ (km s^{-1})	v *sin* i (km s^{-1})	SCZ base
106	29461	21654	0.655	5762	4.505	1.08	1.05	2.2	0.723
109	284574	21741	0.811	5303	4.572	0.95	0.60	4.6	0.697
113	30311	22221	0.560	6107	4.440	1.20	1.41	7.6	0.771
114	30355	22265	0.720	5555	4.540	1.02	0.84	4.1	0.708
115	284787	22350	0.843	5225	4.579	0.94	0.53	2.9	0.694
116	30505	22380	0.833	5249	4.577	1.00	0.80	4.2	0.706
118	30589	22422	0.578	6037	4.454	1.18	1.34	5.8	0.758
119	30676	22496	0.563	6094	4.443	1.20	1.40	14.3	0.769
121	30738	22524	0.536	6202	4.421	1.24	1.51	15.9	0.791
124	30869	22607	0.501	6339	4.393	1.30	1.66	21.6	0.825
127	31609	23069	0.737	5508	4.546	1.00	0.80	3.2	0.706
128	31845	23214	0.450	6558	4.352	1.39	1.89	34.2	0.877
142	30246	22203	0.665	5731	4.511	1.07	1.02	6.6	0.720
143	30809	22566	0.527	6239	4.413	1.26	1.55	10.0	0.801
153	+29 503	13806	0.855	5196	4.582	0.93	0.50	4.0	0.693
162	26874	19870	0.705	5601	4.533	1.03	0.89	1.6	0.711
178	28258	20850	0.839	5235	4.578	0.94	0.54	3.5	0.694
180	28462	20978	0.865	5172	4.584	0.93	0.48	3.9	0.692
187	32347	23498	0.765	5429	4.556	0.99	0.72	4.8	0.702

[a]For stars with no HIP number the B-V photometry is from Joner et al. (2006) except for vB 91 which is from Upgren & Weis (1977).

[b]For stars with no HD number the name is the BD number

Table 4. Li, Be and B Abundances

vB	A(Li)	source[a]	A(Be)[b]	A(B)[c]	A(B)(nLTE)
1	2.96	1	1.39	···	···
2	2.70	1	1.44	···	···
4	<0.43	1	···	···	···
6	3.29	2	···	···	···
8	<1.87	2	···	···	···
9	<0.96	1	1.26	···	···
10	2.73	1	1.12	···	···
11	2.59	2	0.97	···	···
13	<1.70	3	0.61	2.15	2.32
14	3.36	4	1.25	2.50	2.73
15	2.40	4	1.35	···	···
17	1.98	4	1.45	···	···
18	2.53	4	1.42	···	···
19	3.00	2	1.07	···	···
20	3.41	2	···	···	···
21	<0.50	4	···	···	···
26	1.30	4	···	···	···
27	1.65	4	1.44	···	···
31	2.93	4	1.28	···	···
36	1.63	3	···	···	···
37	2.22	3	0.60	2.05	2.24
38	2.89	3	1.16	···	···
39	2.08	1	···	···	···
40	3.19	1	1.44	···	···
42	1.10	4	···	···	···
44	2.41	3	···	···	···
46	<0.53	1	···	···	···
48	3.06	3	1.30	···	···
49	2.47	1	1.42	···	···
51	1.79	3	···	···	···
52	2.73	1	1.42:	···	···

Table 4—Continued

vB	A(Li)	source[a]	A(Be)[b]	A(B)[c]	A(B)(nLTE)
57	2.84	3	···	···	···
59	2.88	2	1.17	···	···
61	3.21	2	1.23	···	···
62	3.12	4	1.19	2.51	2.55
63	2.44	1	1.30	···	···
64	2.30	4	1.46	···	···
65	3.10	4	1.23	2.30	2.38
66	2.76	1	1.13	···	···
69	0.88	1	1.36	···	···
73	2.75	4	1.41	···	···
76	1.14	1	···	···	···
77	2.38	2	1.01	···	···
78	2.64	2	0.87	···	···
79	0.67	5	···	···	···
81	2.23	3	0.93	···	···
85	<1.83	2	···	···	···
86	2.38	3	0.83	···	···
87	1.25	4	1.32	···	···
90	<1.25	2	···	···	···
91	<0.46	1	···	···	···
92	1.24	4	1.32	···	···
93	<0.10	4	···	···	···
94	<0.25	3	···	···	···
96	0.75	1	···	···	···
97	2.65	4	1.22	···	···
99	0.49	1	···	···	···
101	<1.07	2	0.55	···	···
102	2.74	1	···	···	···
105	2.82	1	···	···	···
106	2.45	1	1.38	···	···
109	<0.74	1	···	···	···

Table 4—Continued

vB	A(Li)	source[a]	A(Be)[b]	A(B)[c]	A(B)(nLTE)
113	2.84	4	1.18	···	···
114	1.69	1	1.43	···	···
115	<0.43	1	···	···	···
116	<0.48	1	···	···	···
118	2.74	1	1.44	···	···
119	2.74	1	···	···	···
121	3.15	4	1.28	···	···
124	1.78	3	0.71	···	···
127	1.33	1	···	···	···
128	2.24	3	0.92	···	···
142	2.24	1	···	···	···
143	<1.15	1	···	···	···
153	0.83	1	···	···	···
162	2.16	1	···	···	···
178	0.67	1	···	···	···
180	0.60	1	···	···	···
187	1.38	4	···	···	···

[a]1) Thorburn et al. (1993) equivalent width measures, our new parameters; 2) Boesgaard & Budge (1988) equivalent width measures, our new parameters; 3) Boesgaard & Tripicco (1986) equivalent width measures, our new parameters; 4) Li synthesis in this study; 5) Cayrel et al. (1984) equivalent width measures, our new parameters.

[b]A(Be) from Boesgaard et al. (2004b) synthesis, corrected for our new parameters and for nine of the stars observed for Be here.

[c]All B from synthesized spectra (HST)

Table 5. Boron Abundance Errors due to Uncertainties in the Stellar Parameters

vB	A(B)	ΔT_{eff} ±75 K	Δlog g ±0.20	Δ[Fe/H] ±0.10	Total
13	2.32	±0.04	±0.02	±0.01	±0.05
14	2.73	±0.08	±0.02	±0.03	±0.09
37	2.24	±0.07	±0.02	±0.01	±0.07
62	2.55	±0.04	±0.05	±0.07	±0.09
65	2.38	±0.08	±0.07	±0.04	±0.11

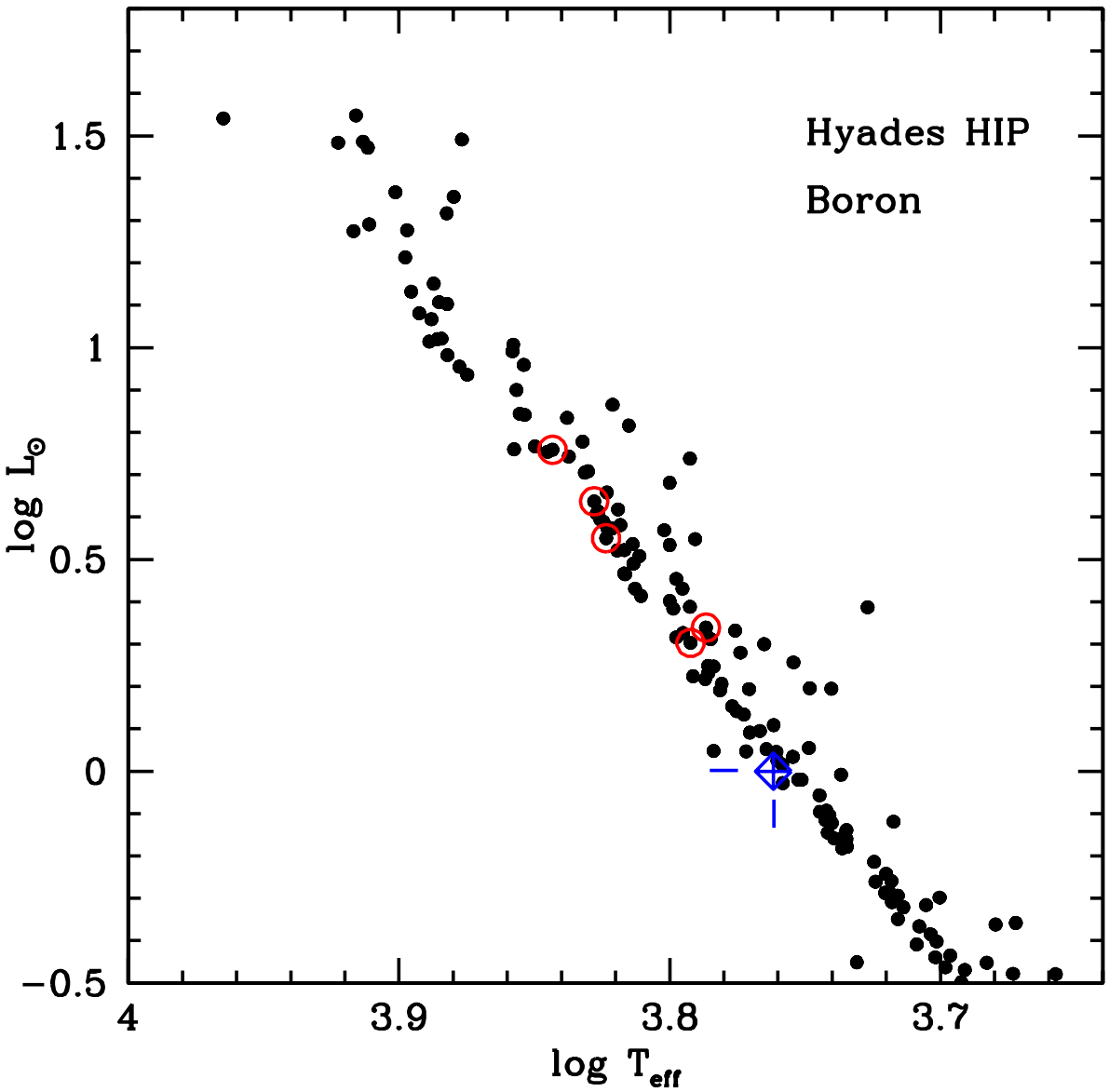

Fig. 1.— The color-magnitude diagram for the Hyades from Hipparcos data showing the positions of the stars observed for B for this program and from the HST archives circled in red. The position of the sun is indicated by the crossed diamond and further delineated by the short vertical and horizontal lines in blue.

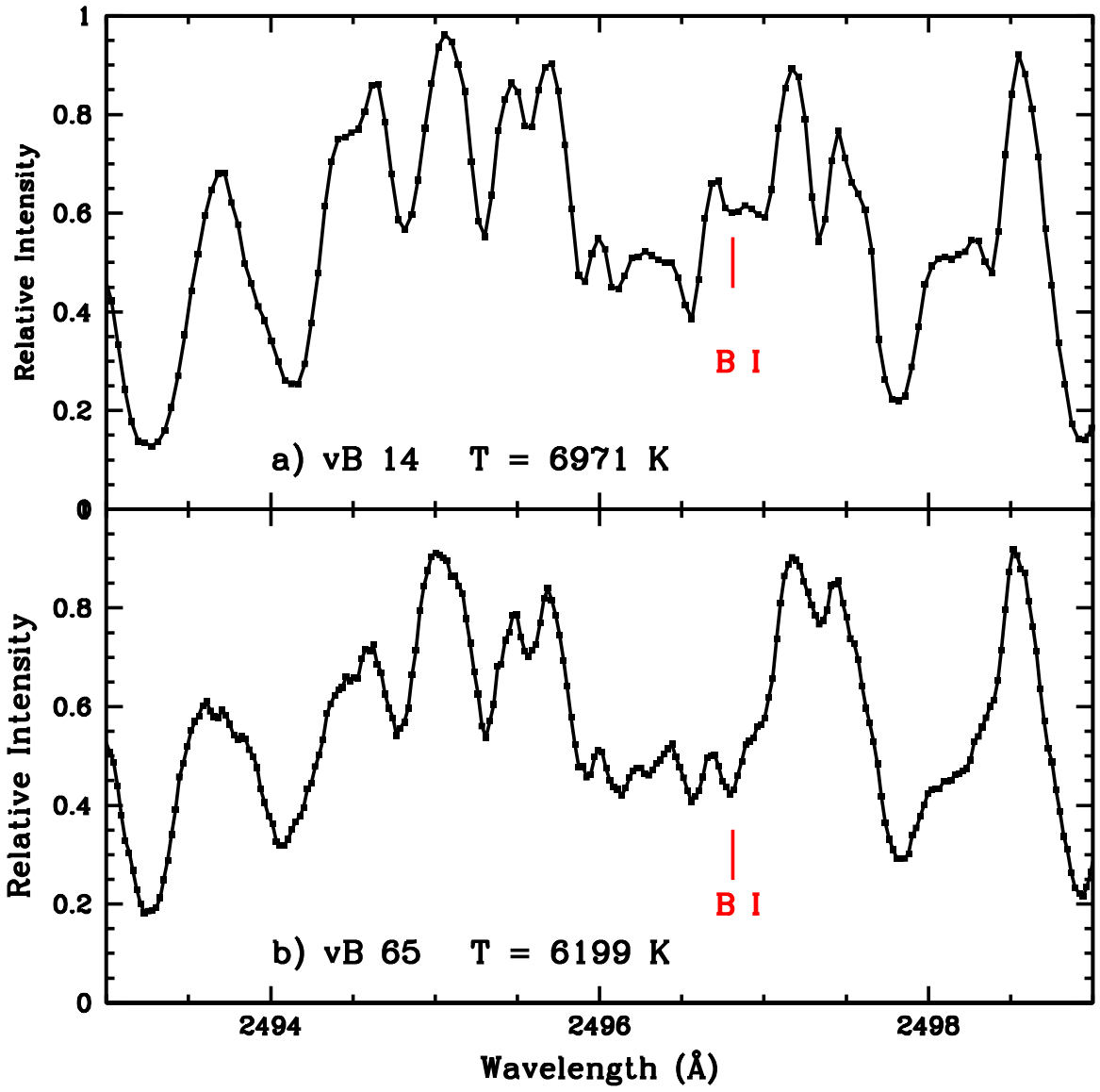

Fig. 2.— The spectra of two of our stars in the B I region, indicating the B I line that we used in the B abundance analysis.

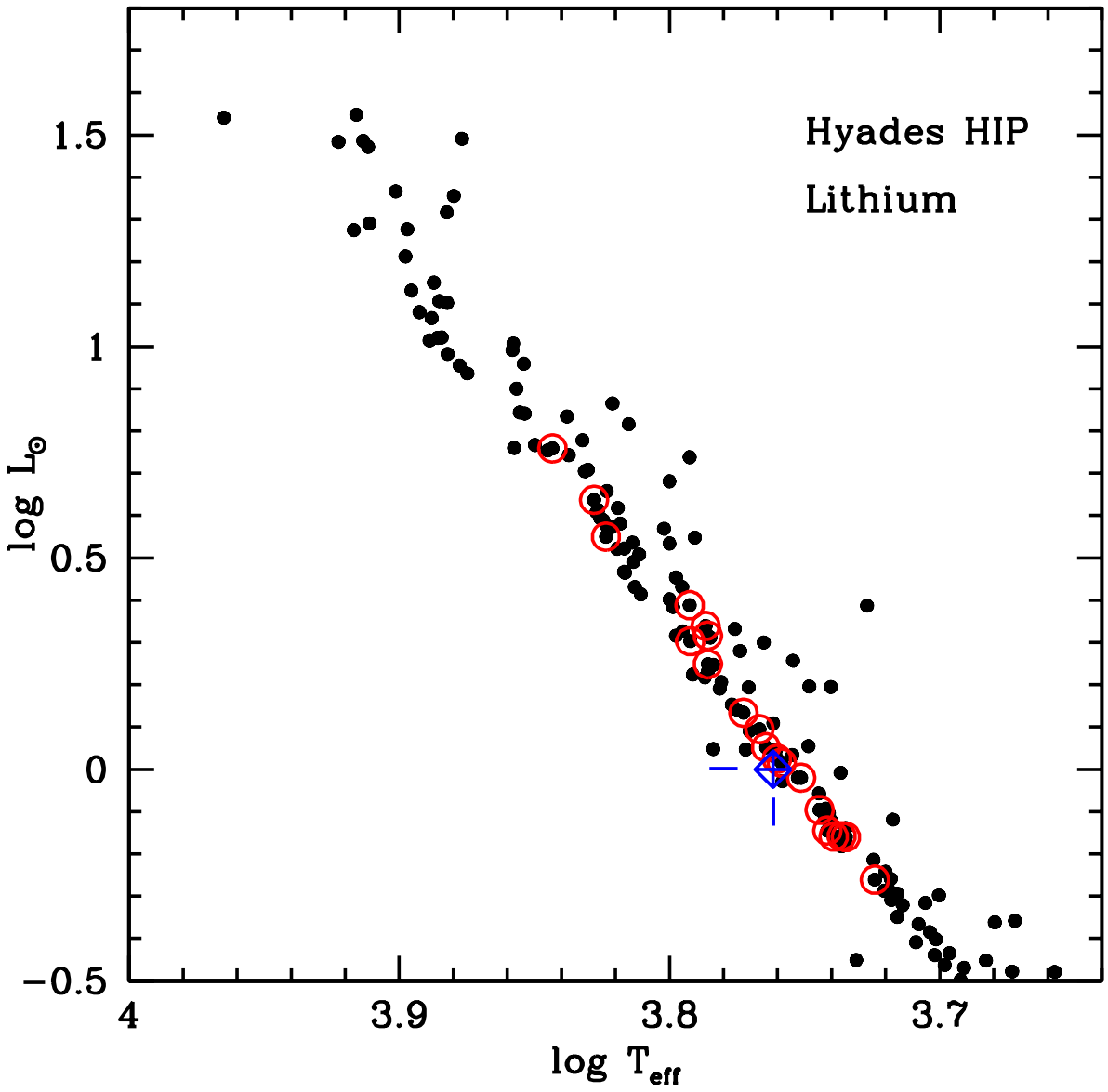

Fig. 3.— The color-magnitude diagram for the Hyades from Hipparcos data. The stars newly observed for Li are circled. As in Figure 1 the position of the Sun is indicated.

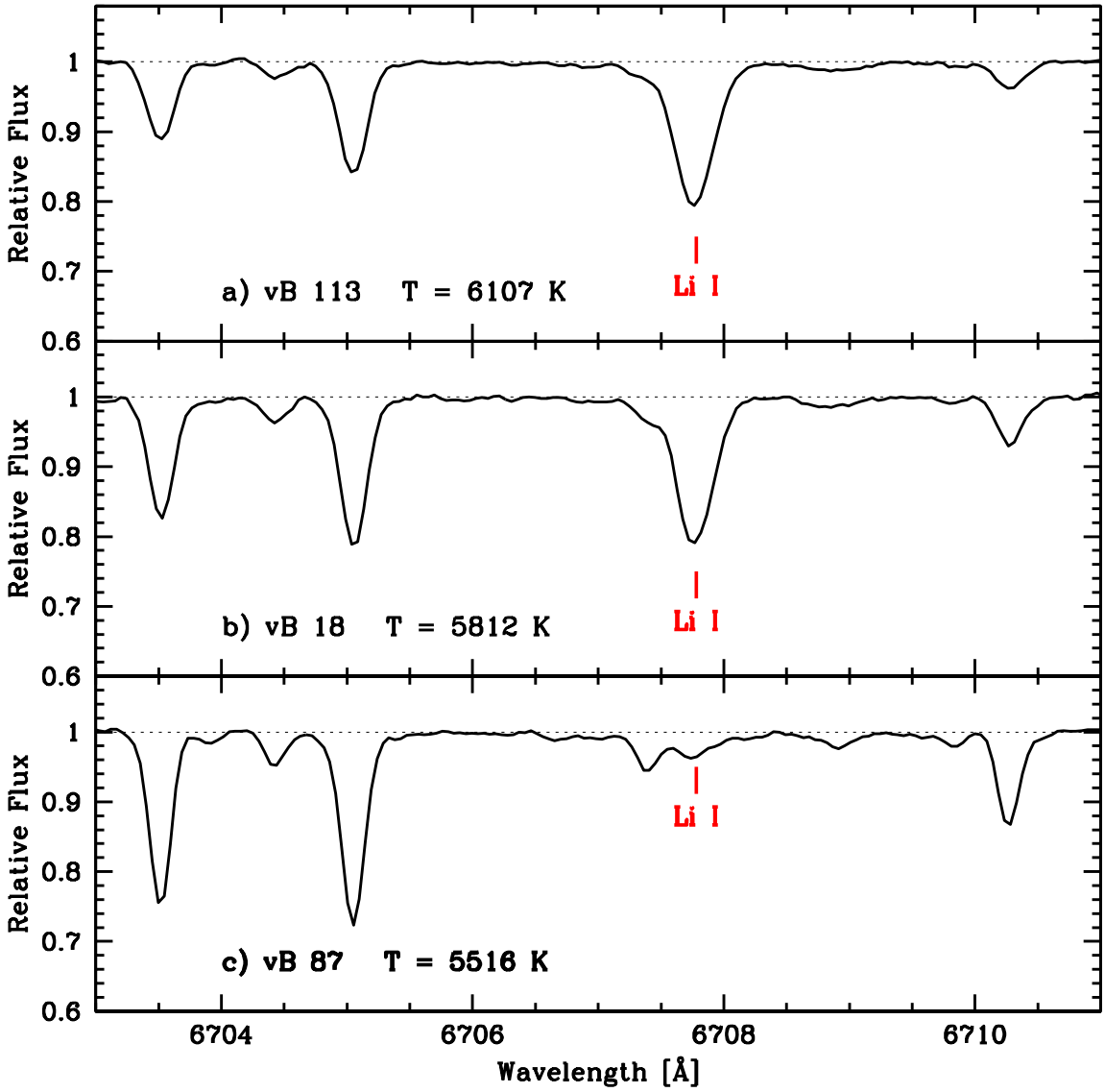

Fig. 4.— A region eight Å in the spectra of three stars near the Li I line at λ6707. The three stars show a range in temperature and the Li I doublet is obviously much weaker in the coolest star. It is very depleted in Li.

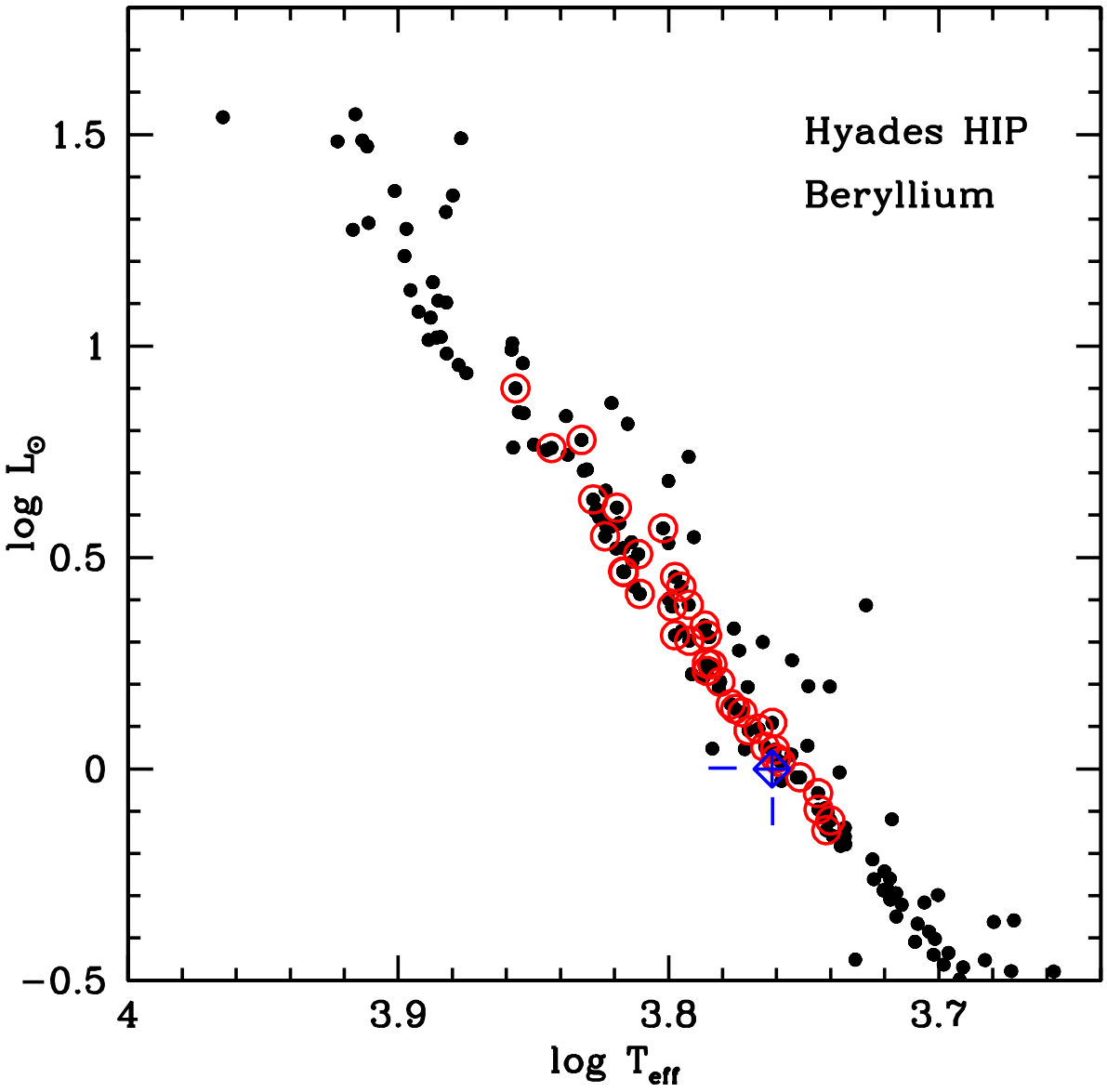

Fig. 5.— The color-magnitude diagram for the Hyades from Hipparcos data showing the positions of the stars observed for Be by Boesgaard and King (2002) and in this work. As in Figure 1 the position of the Sun is indicated.

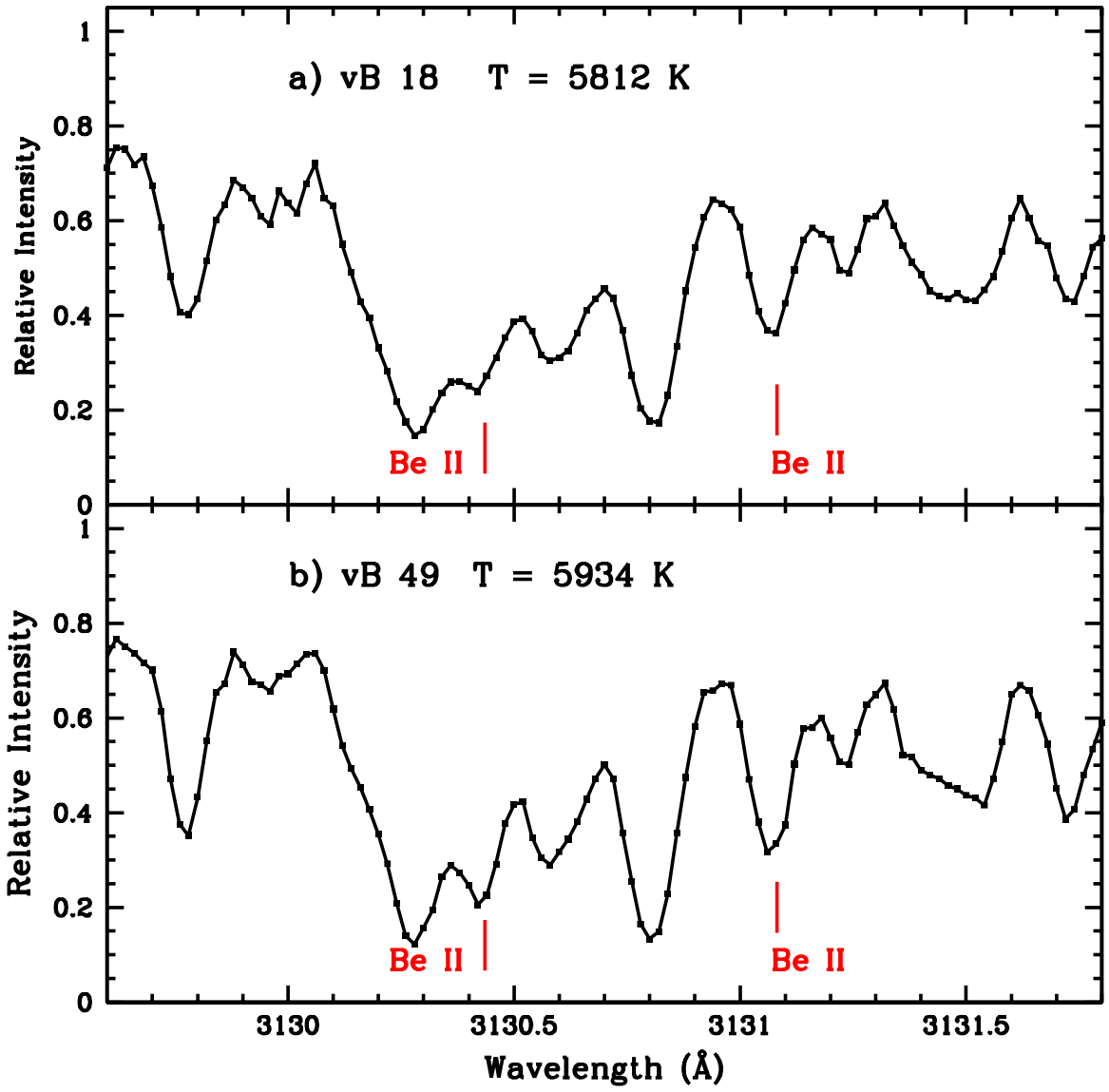

Fig. 6.— The spectra of Be for two of our new observations

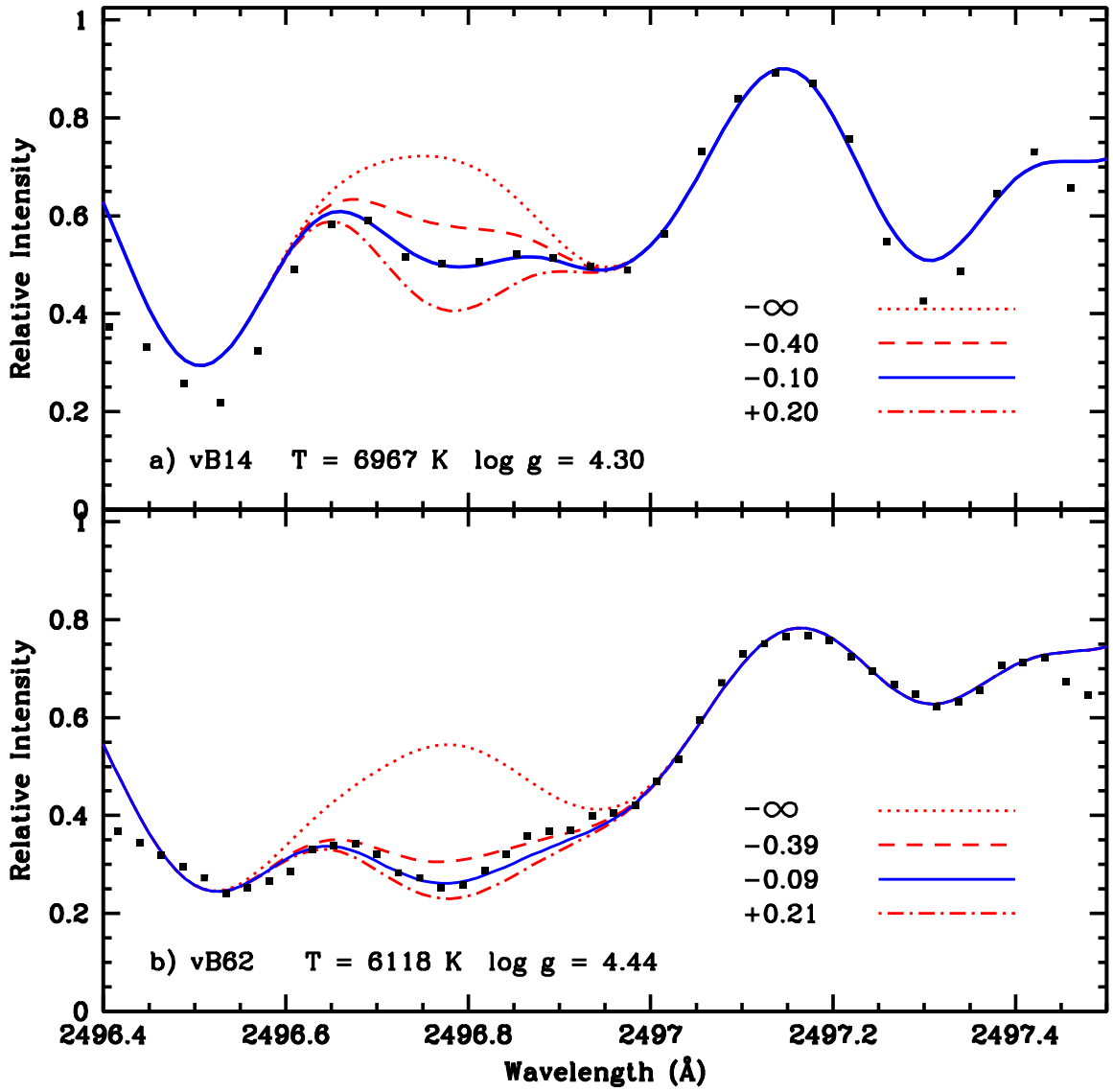

Fig. 7.— The synthesis fits for B in vB 14 and vB 62. The observations are the black squares. The best fit synthesis is shown by the blue line. The B abundance of a factor of 2 larger is shown as the red dot-dash line and a factor of 2 smaller by the red dashed line. The synthesis with no B is the red dotted line.

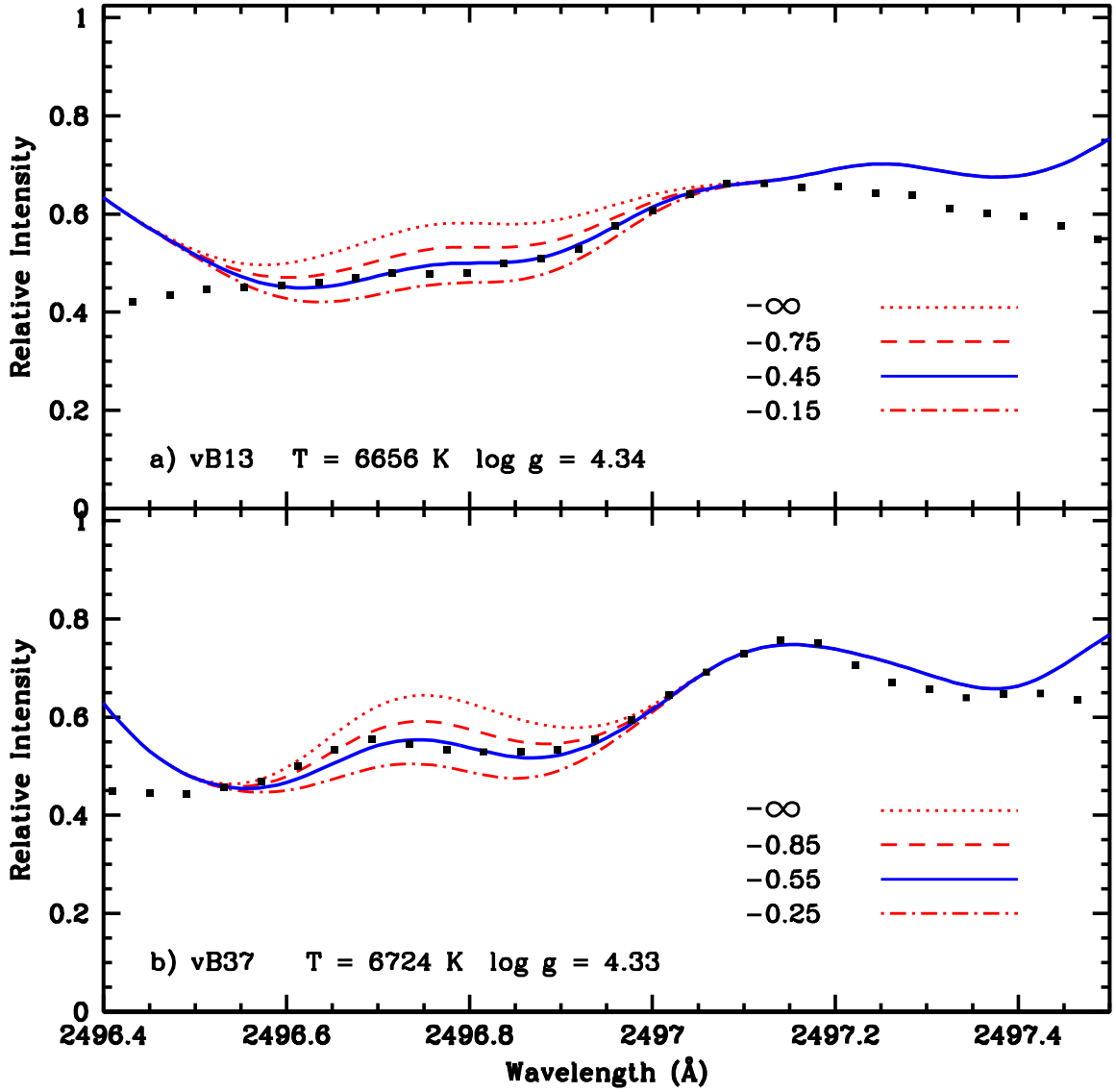

Fig. 8.— The synthesis fits for B in the two Li-Be dip stars, vB 13 and vB 37. The lines and symbols are the same as in Figure 7.

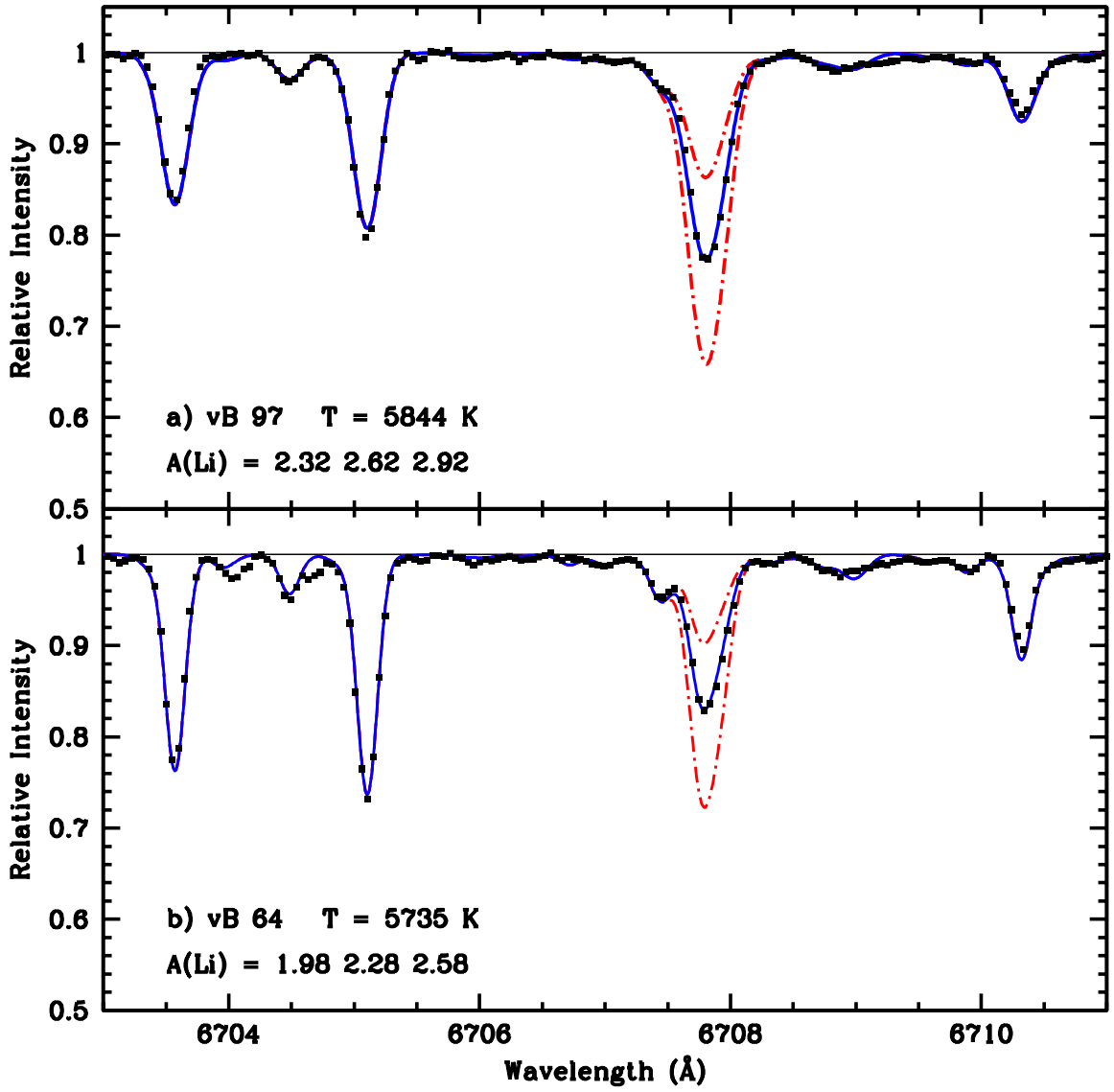

Fig. 9.— Example of the Li synthesis for vB 97 and vB 64. The observations are the black squares. The best fit synthesis is shown by the blue line. Abundances of Li a factor of 2 larger and smaller are shown by the red dash-dot line. The position of the continuum is the narrow black line at 1.00.

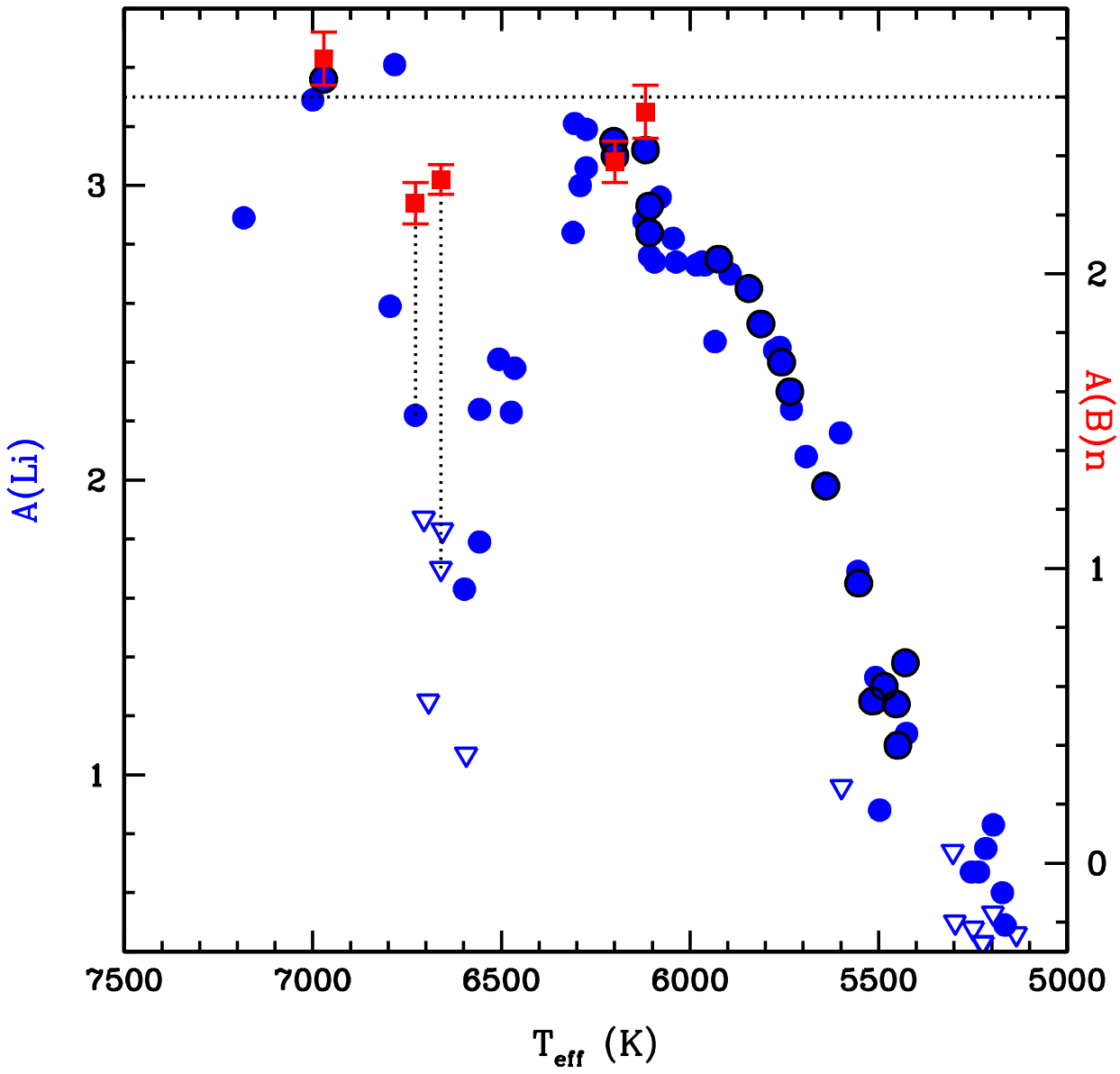

Fig. 10.— The Li-temperature profile for the Hyades F and G stars. The blue filled circles are Li detections while the blue open triangles are Li upper limits. The Li abundances from the Li observations reported in this work are circled in black. Note the pronounced drop in Li abundances in the range 6400 - 6850 K, the Li "dip." The Li abundances also drop sharply in the cooler G stars with T < 6000 K. The data are from this paper, Boesgaard & Tripicco (1986), Boesgaard & Budge (1988), and Thorburn et al. (1993) (as reanalyzed here with the Hipparcos parameters from de Bruijne et al. (2001)). The B results - all detections - are the red filled squares. The abundances are shown on the same scale and normalized to the solar system abundances of Li and Be (Grevesse & Sauval 1998) as indicated by the horizontal dotted line. There are two stars in the Li dip that appear to be deficient in B; these are connected to their Li values by dotted lines.

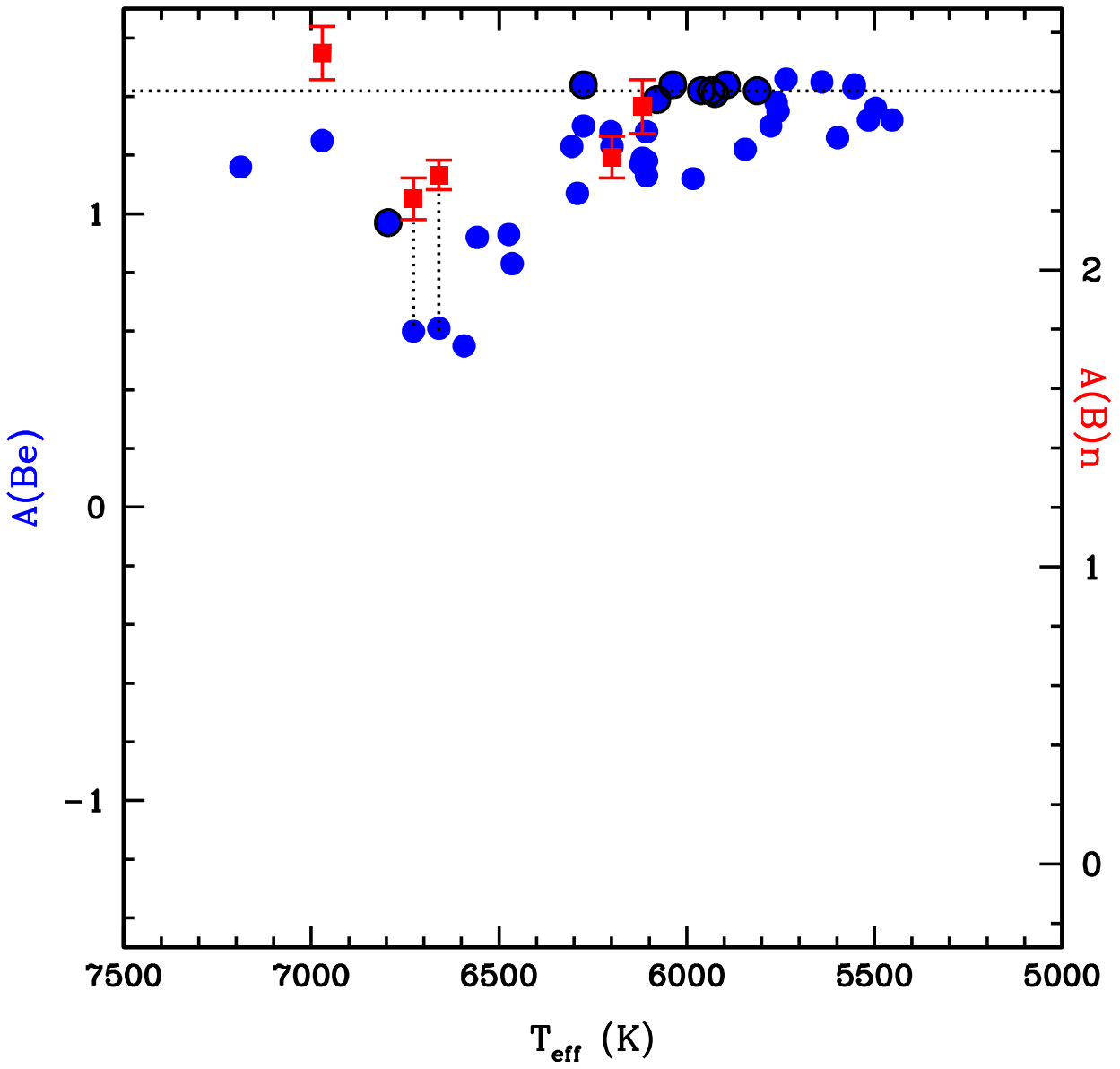

Fig. 11.— The Be-temperature profile for the Hyades F and G stars, on the same vertical scale as the Li plot in Figure 10. The blue filled circles are the Hyades Be abundances. The Be abundances from the Be observations reported in this work are circled in black. There are Be deficiencies in the same temperature region as the Li deficiencies. Unlike the Hyades Li abundances, there are no Be deficiencies in the G stars. The data are from Boesgaard & King (2002) (as reanalyzed in Boesgaard et al. 2004a and adjusted for the Hipparcos parameters used here) and from the new Be observations presented here. The B results are shown as filled red squares on the same vertical scale as A(Be) and as A(Li) in Figure 10. The horizontal dotted line corresponds to the meteoritic/solar values of Be and B. There are two stars in the Be dip that appear to be deficient in B; these are connected to their Be values by dotted lines.

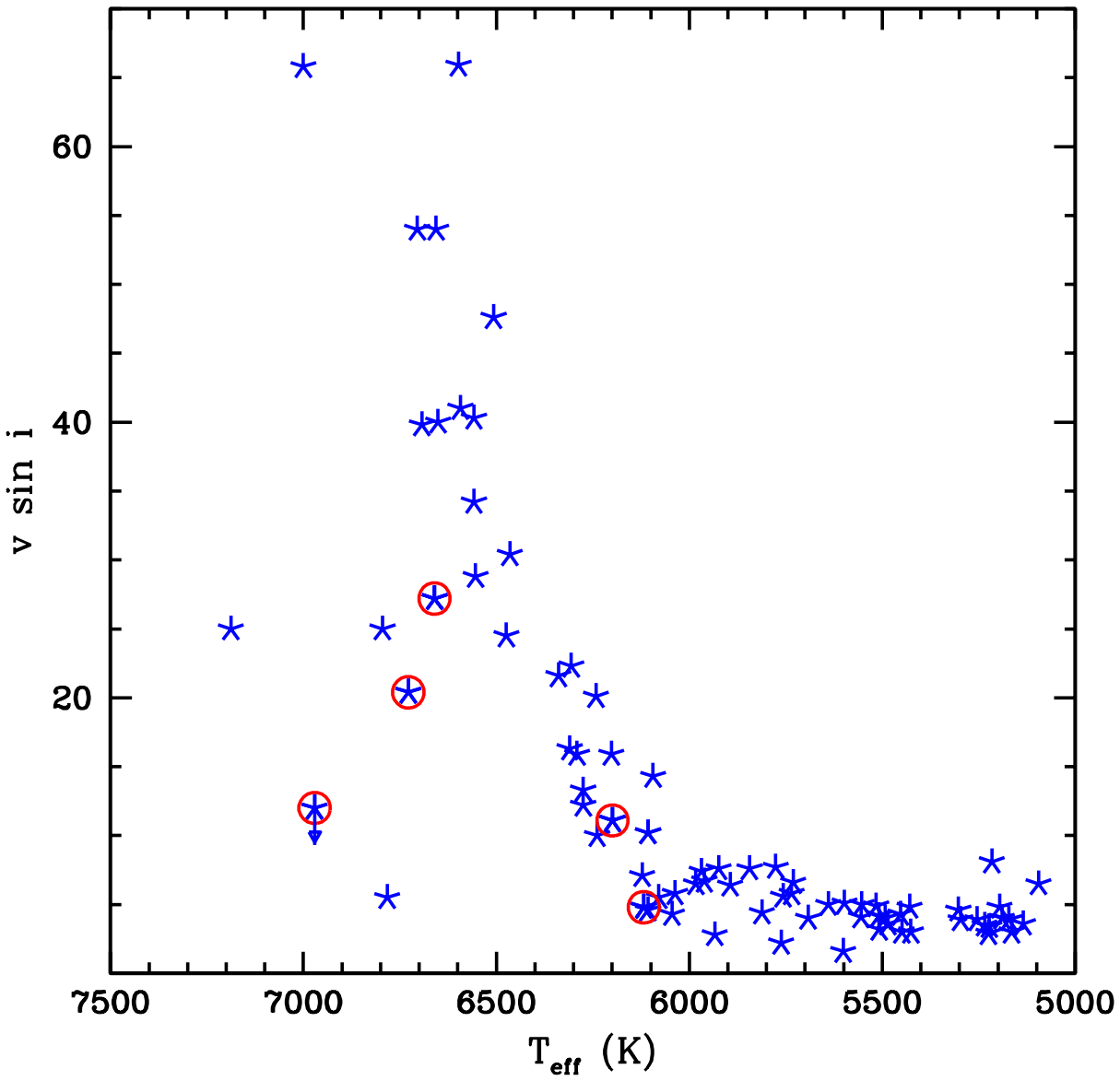

Fig. 12.— The measured vales of v *sin* i given in Table 3 are shown as a function of $T_{\rm eff}$. A dramatic drop is found from 6800 to 6200 K. The points for the five stars observed for B are circled in red.

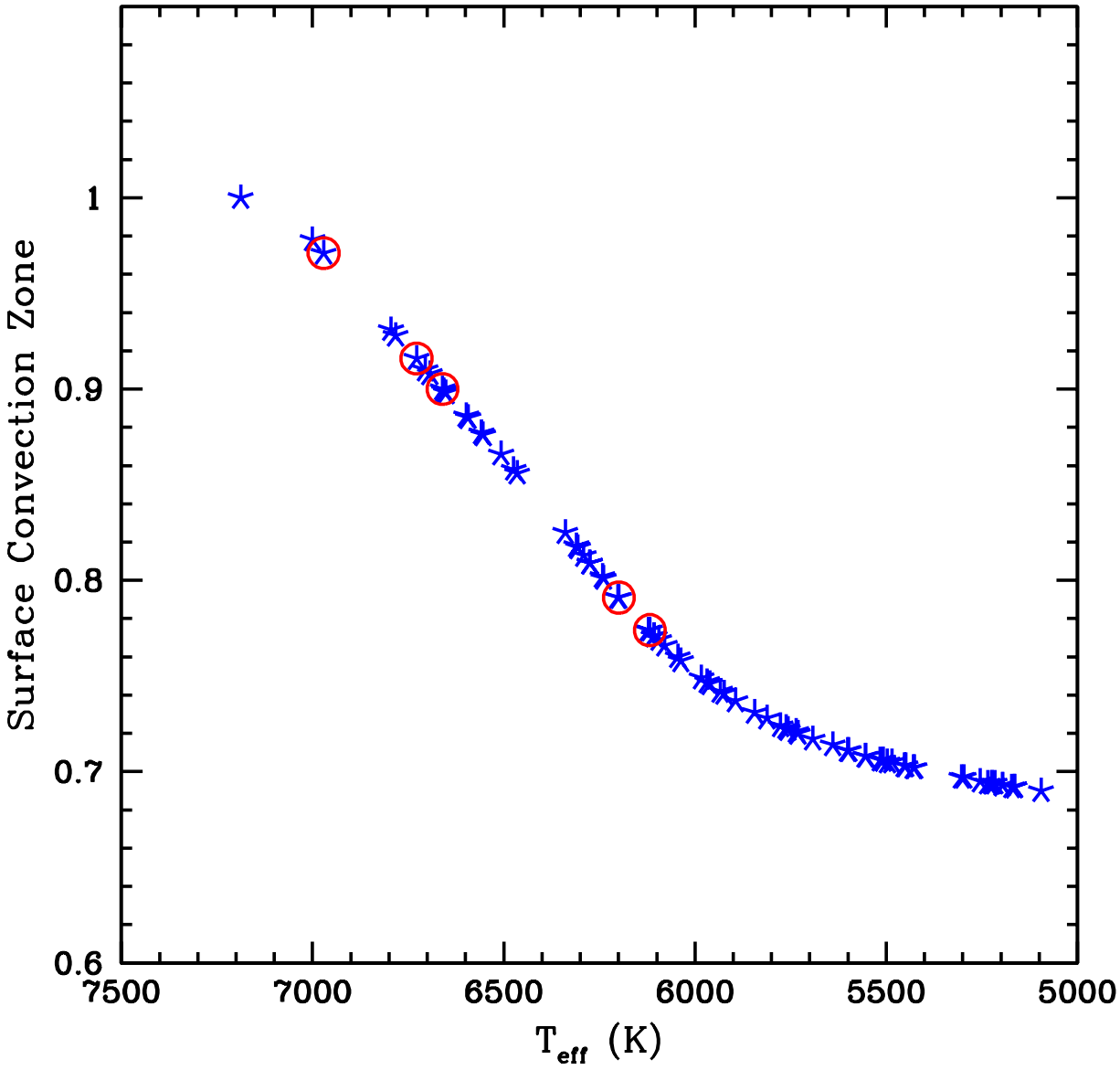

Fig. 13.— The depth of the SCZ with respect to the fractional radius, where the surface is 1.0 as a function of the stellar surface temperature. The y-axis corresponds to the boundary between the SCZ and the radiative layer. There is no SCZ for the hottest stars. It deepens smoothly toward cooler stars and reaches down to ∼30% of the star by 5500 K. The points for the five stars observed for B are circled in red.

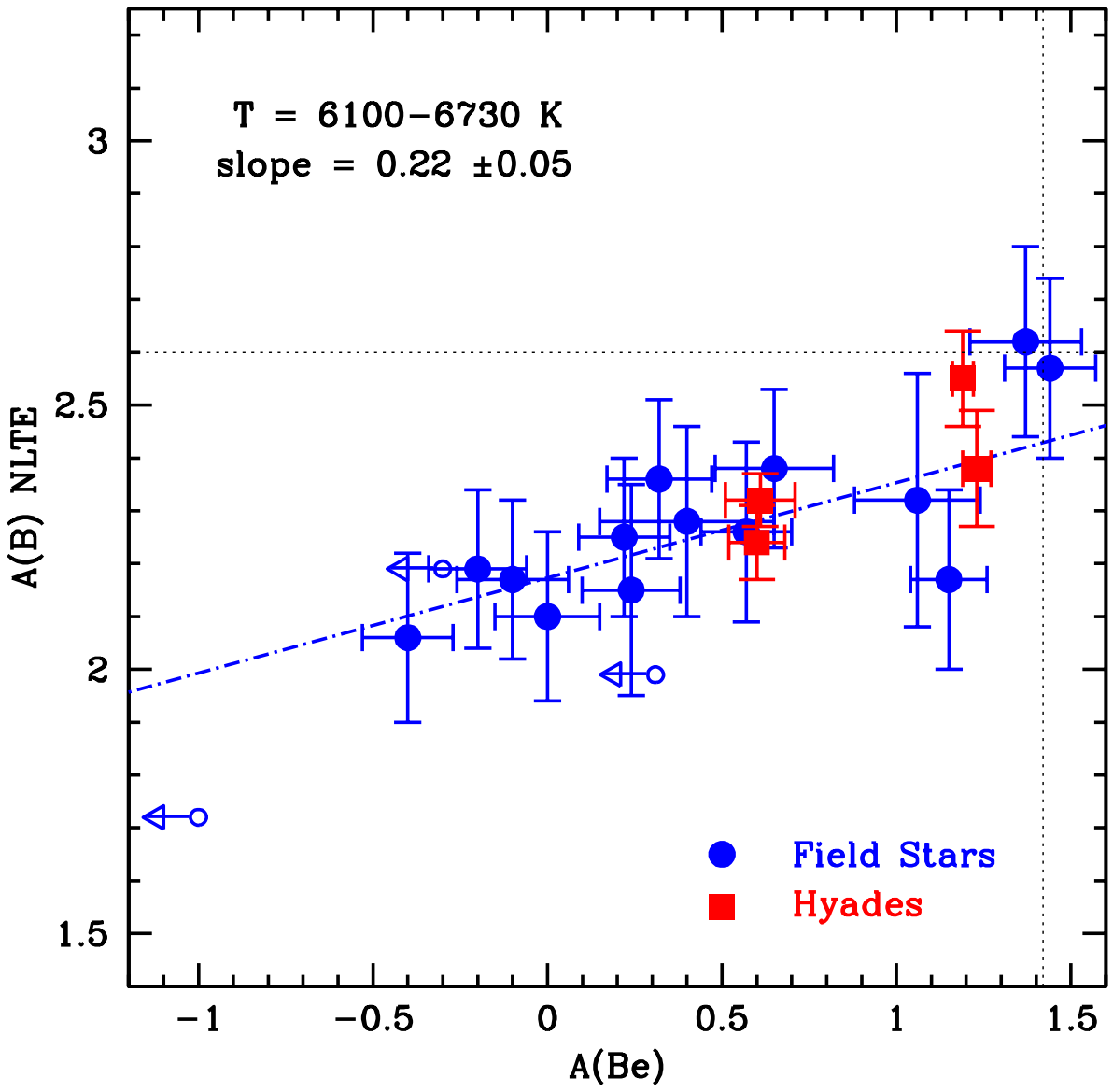

Fig. 14.— The correlation of Be and B abundances in stars on the cool side of the Li-Be dip. The field star data are from Boesgaard et al. (2005). The four cool Hyades stars fit very well with the correlation from the field stars. The dotted black lines show the initial Be and B abundances.

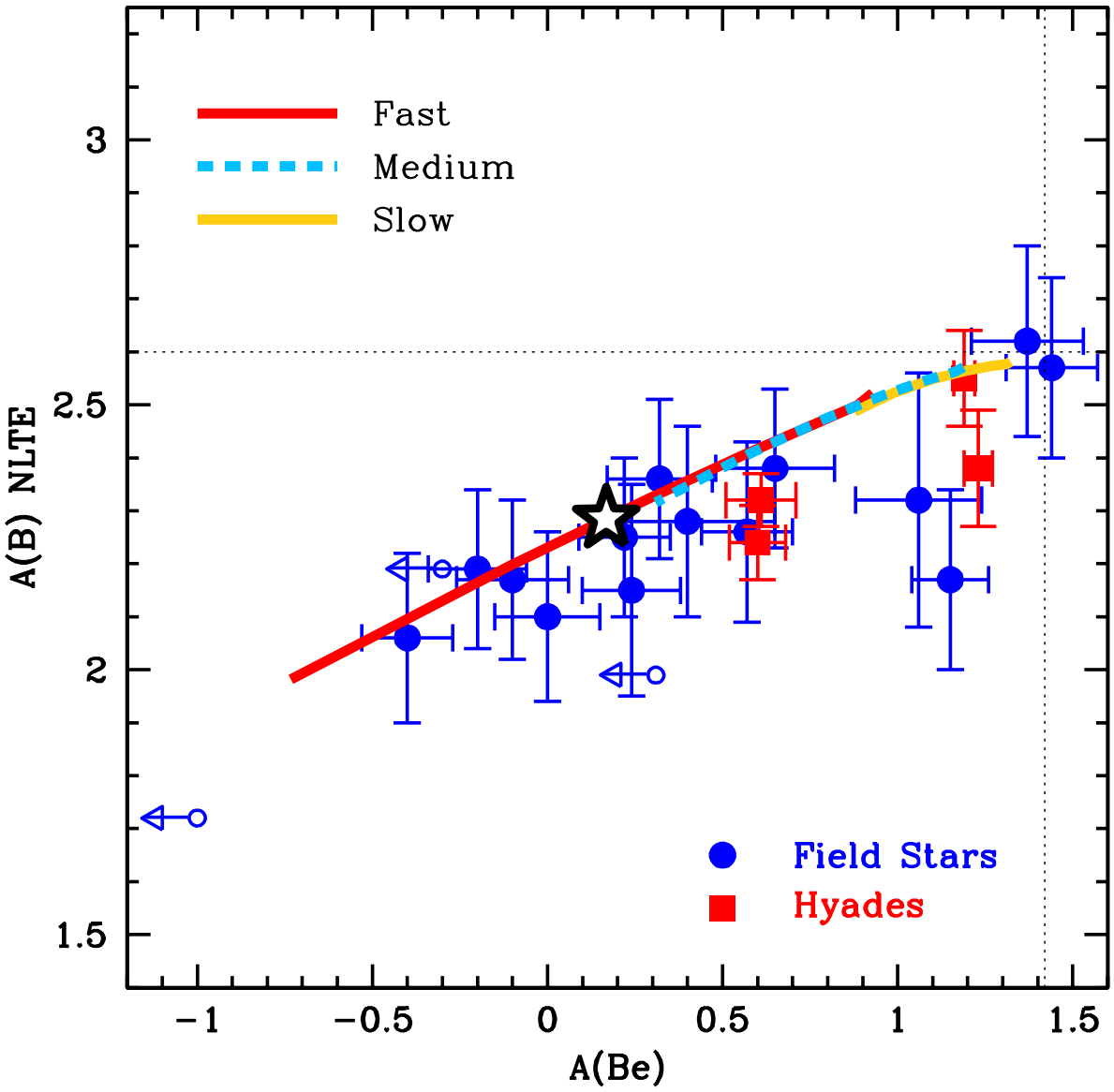

Fig. 15.— Data points same as Figure 14, with fast, medium, and slow rotational mixing models run to 2 Gyr over-plotted. The dotted black lines show the initial Be and B abundances of the mixing calculations. The models reproduce well the slope of the Be-B correlation, though are more rich in B by about 0.1 dex compared to the Hyades stars. The black star marker reflects the most depleted model at 700 Myr, suggesting sufficient B depletion can be driven by rotational mixing at the age of the Hyades.